MEASUREMENTS OF ISOLATED PROMPT PHOTONS IN pp COLLISIONS WITH THE ATLAS DETECTOR

Francesco Polci (LPSC Grenoble)
on behalf of the ATLAS Collaboration

Europhysics Conference on High-Energy Physics (EPS-HEP 2011, Grenoble)

MOTIVATIONS

SINGLE PHOTON

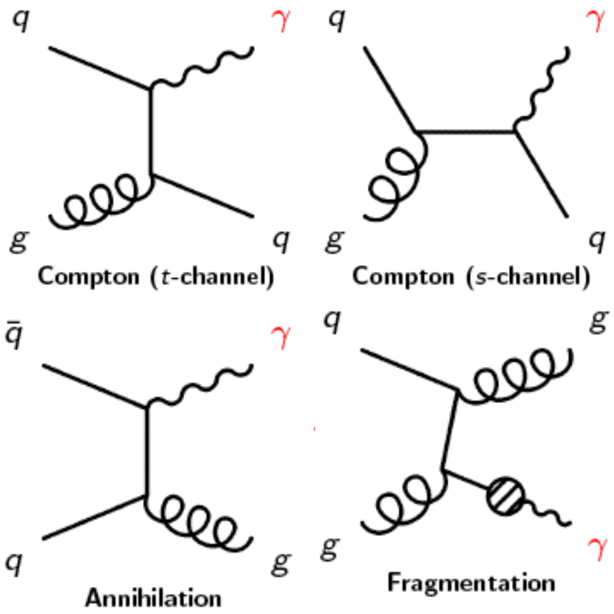

- Compton dominant process.
- Fragmentation, giving photons closer to hadrons, important at low E_T

DI-PHOTONS

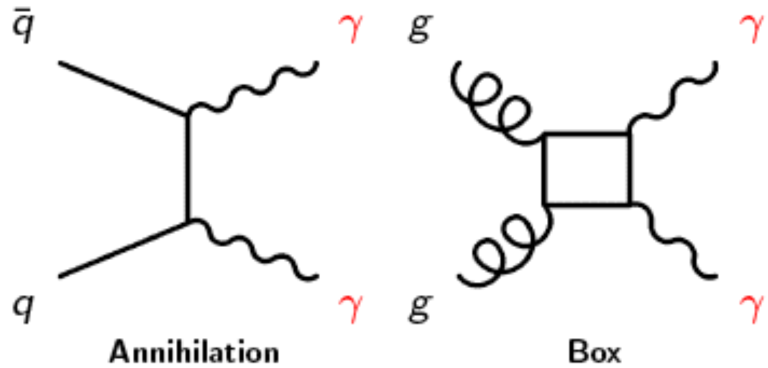

- Annihilation and box comparable due to high gluons flux at LHC

PHOTONS MEASUREMENTS AT HADRON COLLIDERS:

- test of perturbative QCD
- sensitive to the gluon content of the proton
- allow to estimate QCD background for *Higgs*, *Graviton*, *excited fermions* and *pairs of supersymmetric particles* searches

PHOTON RECONSTRUCTION AND IDENTIFICATION
(ATL-PHYS-PUB-2011-007)

PHOTON IDENTIFICATION

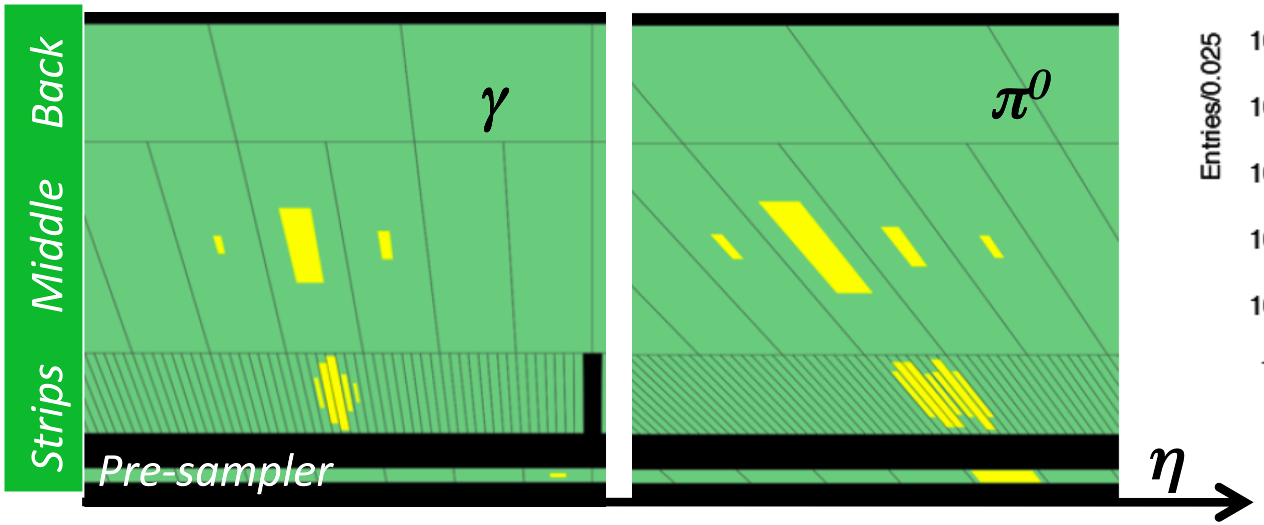

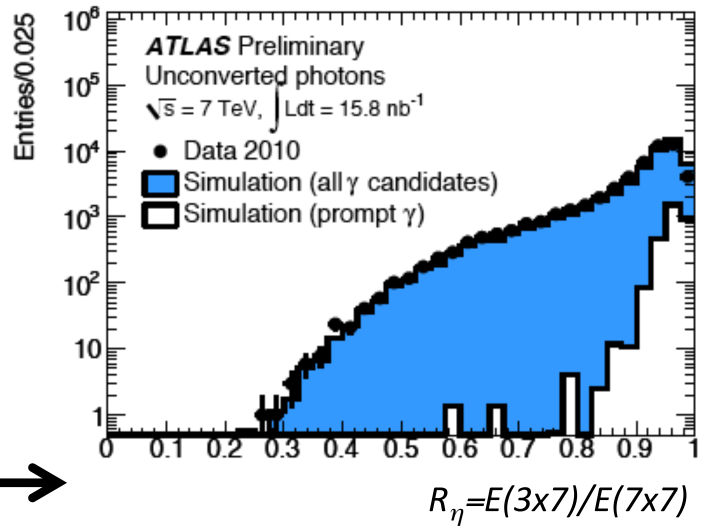

- ***Loose selection***:
  - small energy in the hadronic calorimeter;
  - narrow showers in the middle sampling.

- ***Tight selection***:
  - tighter cuts in the middle sampling;
  - cuts on strip variable (rejecting π^0).

- About ***30% of photons converted*** in ATLAS:
  - the tracker informations are also used;
  - dedicated cuts optimization.

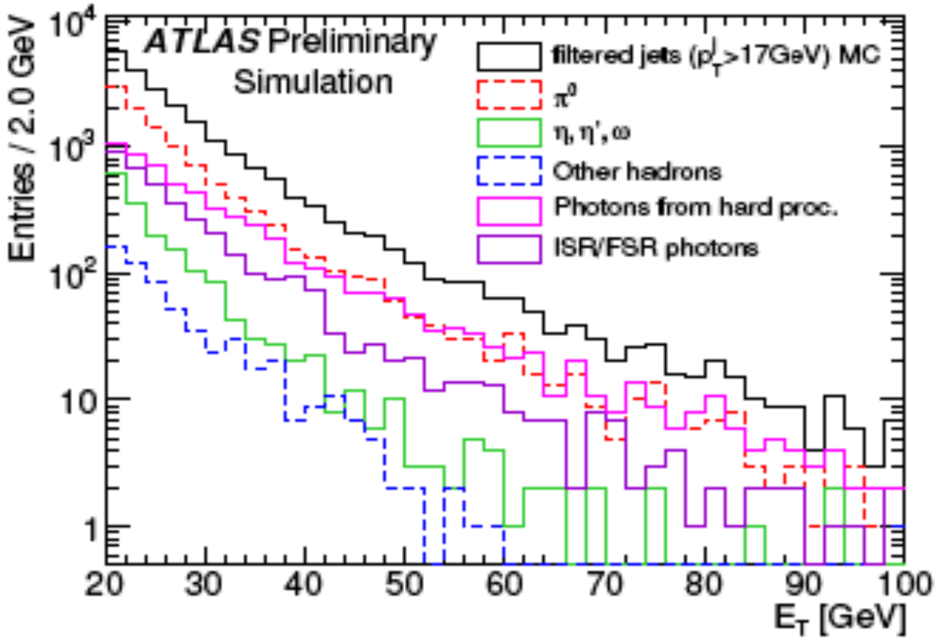

CALORIMETER ENERGY ISOLATION: E_T^{ISO}

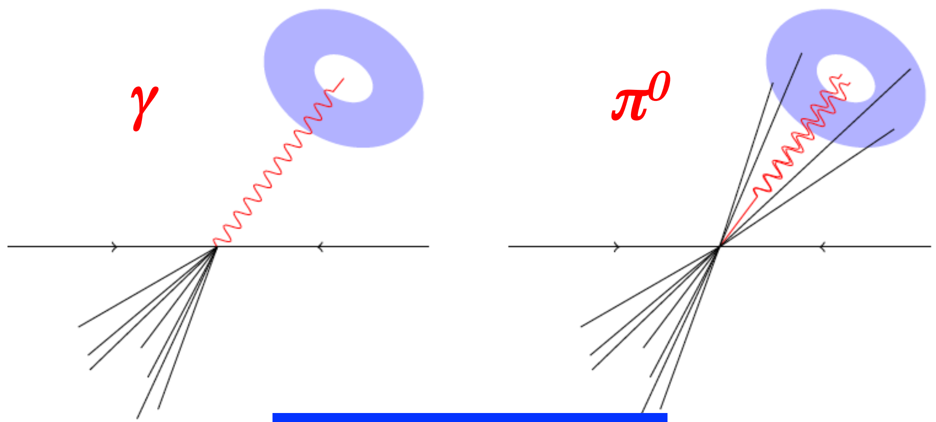

ISOLATION ENERGY

$$E_T^{ISO} = \sum_{cells} E_T \quad \text{in} \quad \Delta R = \sqrt{(\Delta\eta)^2 + (\Delta\phi)^2} < 0.4$$

subtracting:

- energy of the cluster;
- signal energy leakage out-of-cluster;
- soft-jet activity from pileup and underlying event (~500 MeV).

Impact of the isolation cut:

- lower QCD backgrounds;
- reduced fragmentation contribution.

Data driven methods for isolation shape!

1) Determine background E_T^{ISO} shape reversing tight cuts.

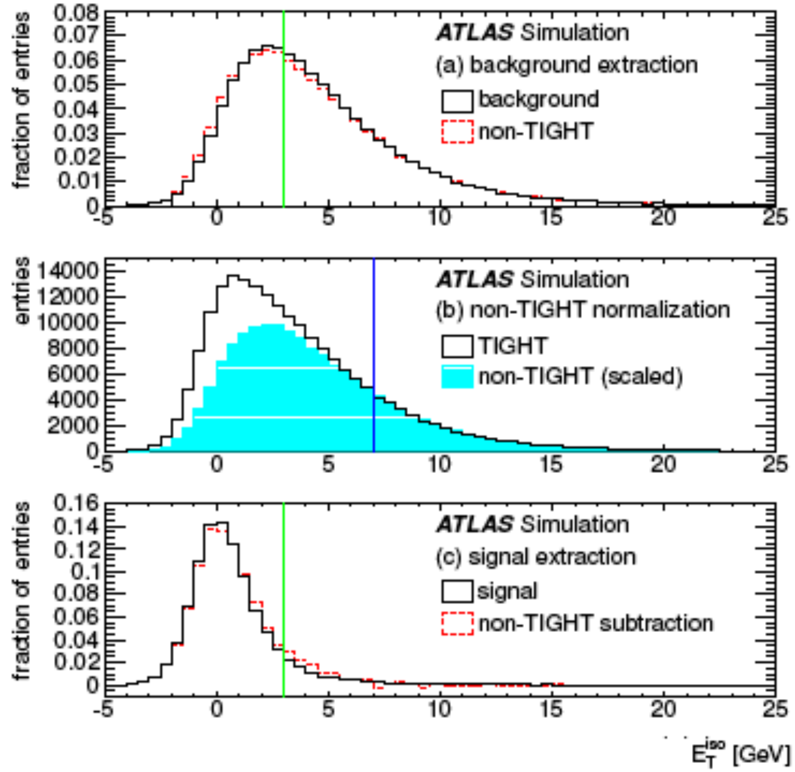

2) Extract photon isolation shape in $e^{\pm}$ from *W,Z*, correcting for e/γ differences.

PHOTON EFFICIENCY

- ***Trigger efficiency***: 100% for γ passing offline selection

- ***Reconstruction efficiency***: ~85% in barrel, ~70% in end-cap
  - main losses due to dead readout recovered in 2011

- ***Tight plus isolation efficiency:***
  - from Monte Carlo γ sample;
  - shower shapes shifted according to comparison with data;
  - data driven cross-check with in $e^{\pm}$ from *W,Z*

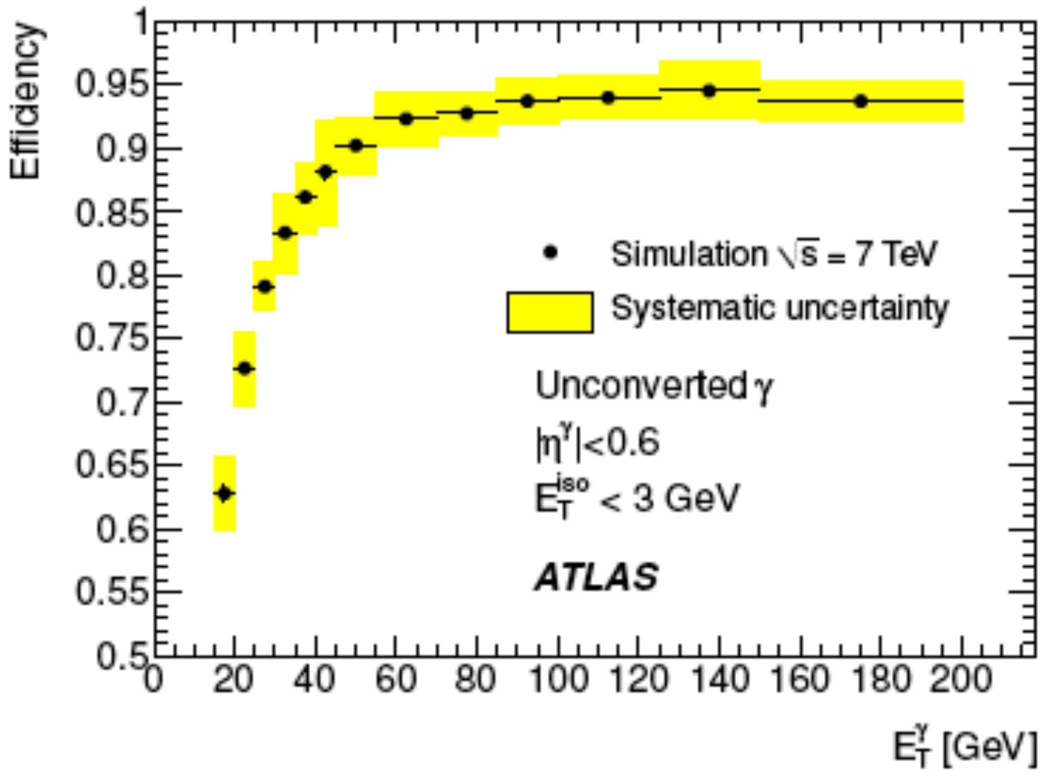

INCLUSIVE ISOLATED PROMPT PHOTON CROSS-SECTION MEASUREMENT @ $\sqrt{s}$= 7 TeV

- Phys. Rev. D83, 052005 (2011): $L = 0.85\ pb^{-1}$, $15 < E_T(\gamma) < 100$ GeV
- ATLAS-CONF-2011-058: $L = 35\ pb^{-1}$, $45 < E_T(\gamma) < 400$ GeV

BACKGROUND DETERMINATION: SIDEBANDS METHOD

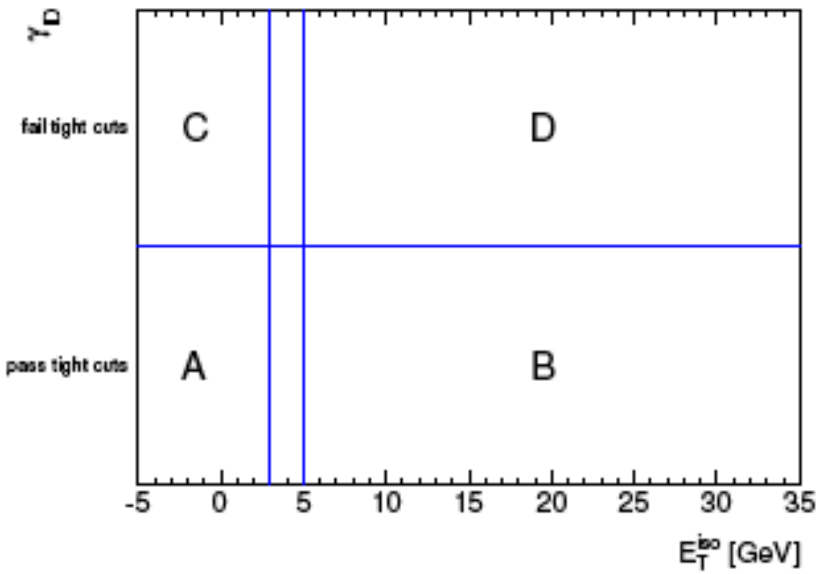

- A = signal region
- B, C, D control regions
- Hypothesis:
  1) B, C, D background dominated: $N^{\rm bkg}_{B,C,D} \simeq N_{B,C,D}$
  2) negligible correlation between tight ID and E_T^{ISO}:

$$\frac{N_A^{\rm bkg}}{N_C^{\rm bkg}} \simeq \frac{N_B^{\rm bkg}}{N_D^{\rm bkg}}$$

$$\boxed{N_A^{\rm sig} = N_A - N_A^{\rm bkg} \simeq N_A - \frac{N_B N_C}{N_D}}$$

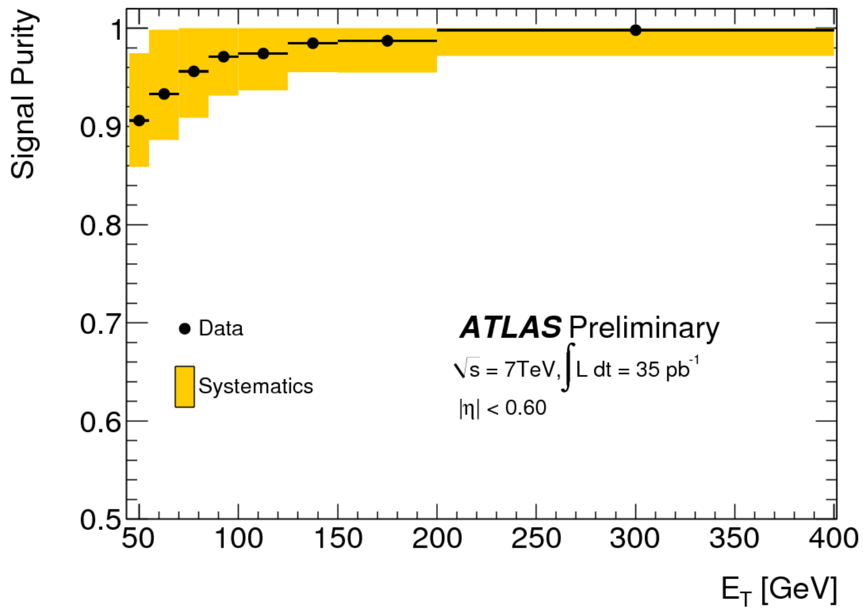

- Isolated electron contamination estimated from data and Monte Carlo samples

BACKGROUND DETERMINATION: ISOLATION TEMPLATES METHOD

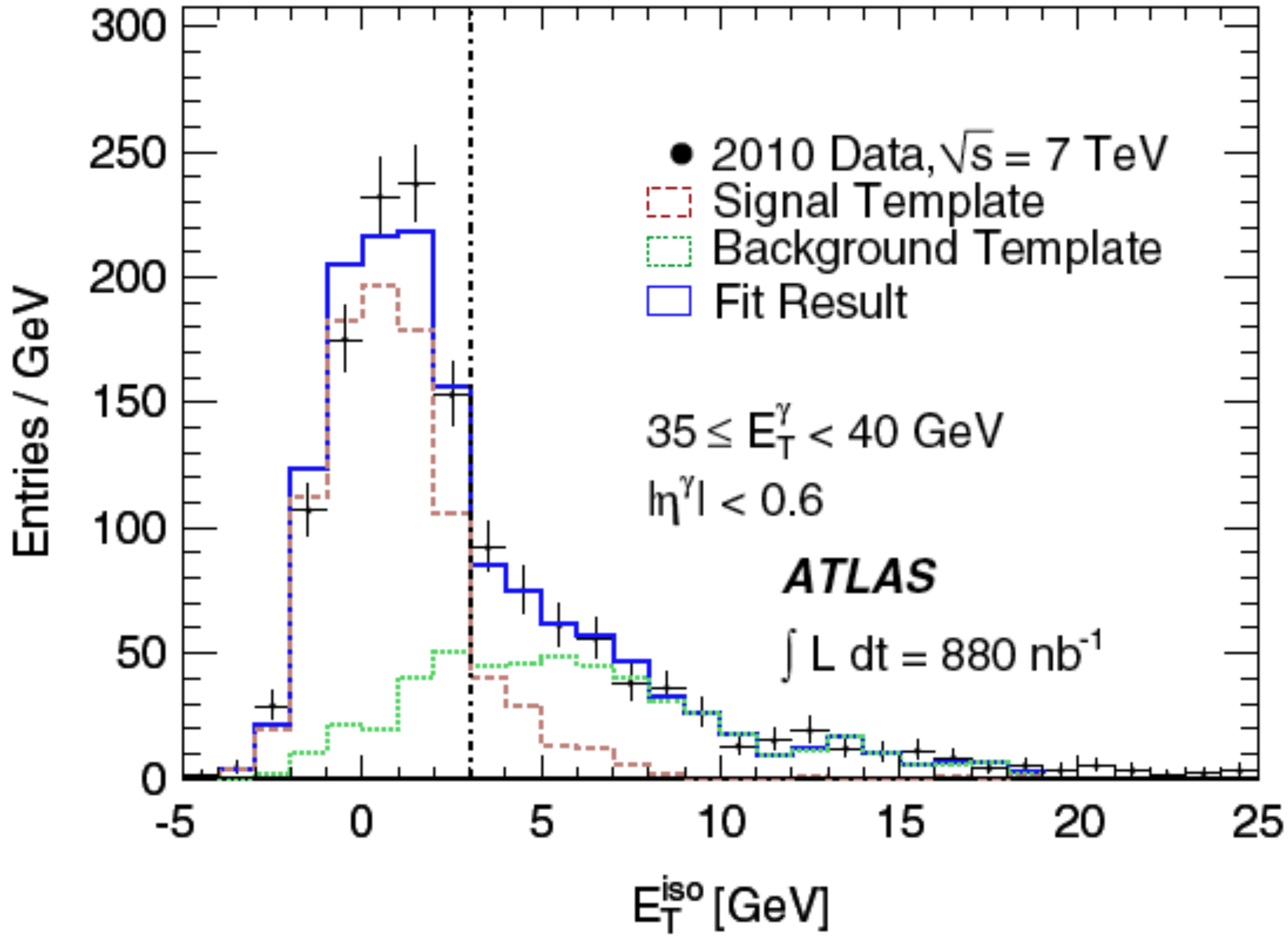

- Signal template from $e^{\pm}$ from *W* and *Z*, correcting for e/γ shift with simulations
- Background template from data reversing tight ID criteria.
- Results in agreement with sidebands method within 2%

INCLUSIVE ISOLATED PROMPT PHOTON PRODUCTION CROSS SECTION 1

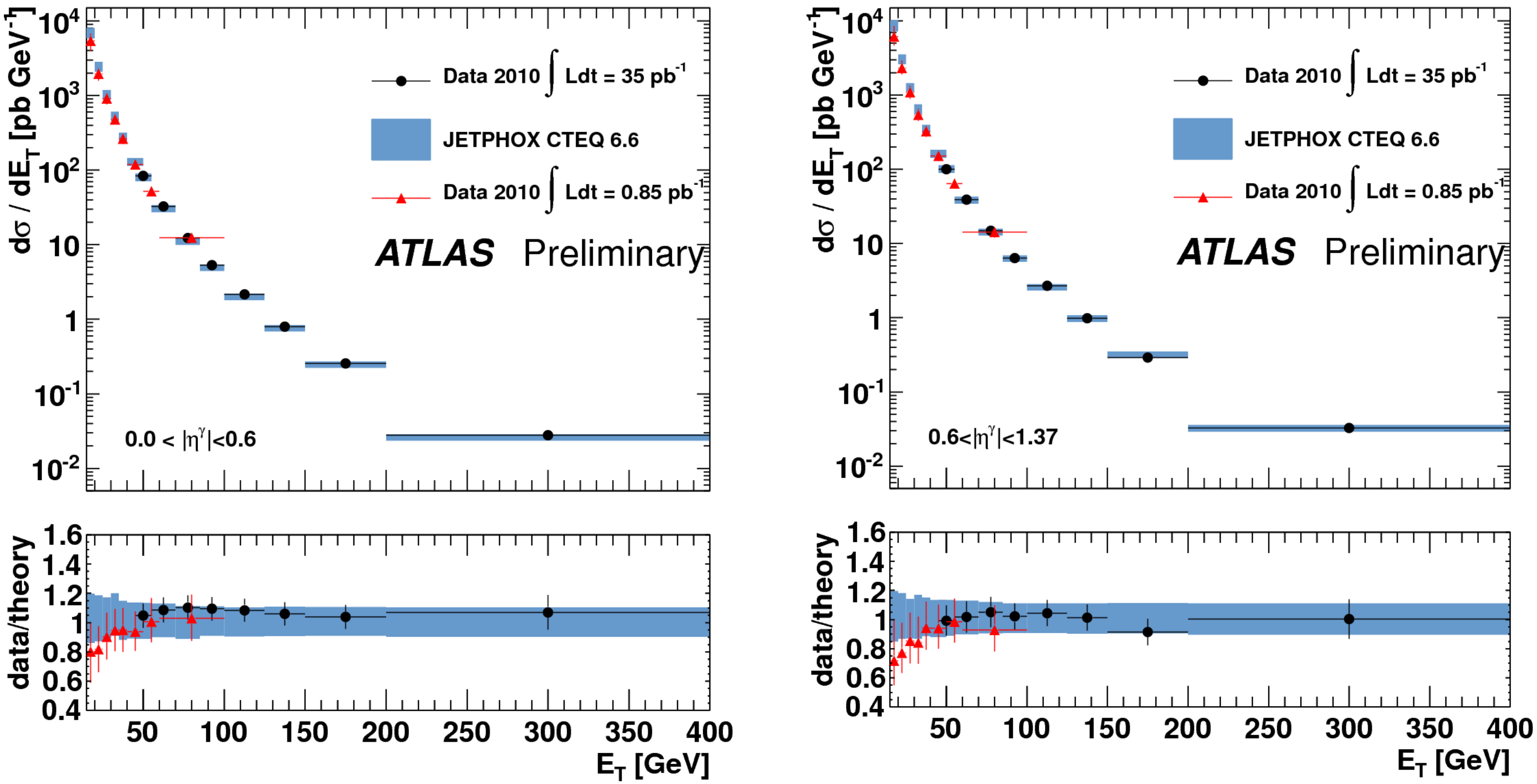

- Unfolding from E_T response matrix (bin-by-bin, iterative, SVD)
  - largest experimental systematics: EM energy scale (3% in test beam, 1.5% from Z)
    => 5-10% on cross-section
- Comparison to NLO pQCD prediction by JetPhox CTEQ 6.6
- Good agreement, except in E_T<35 GeV (region of higher fragmentation contribution)

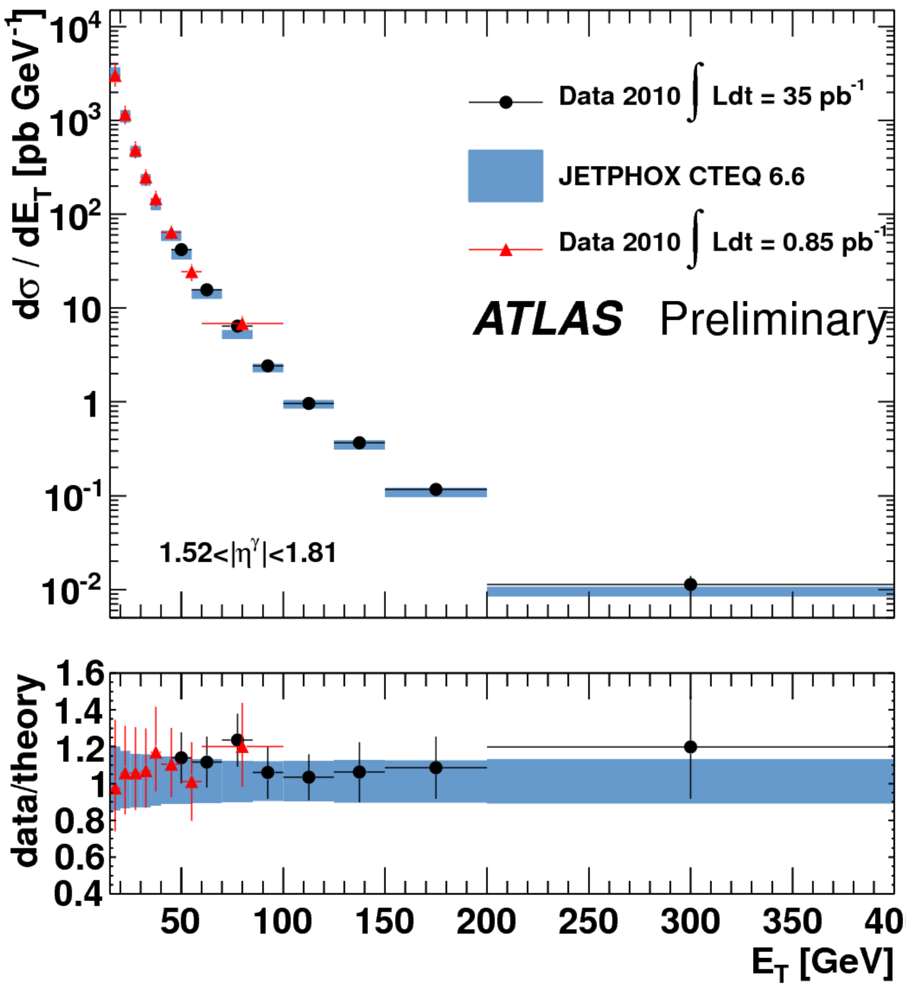

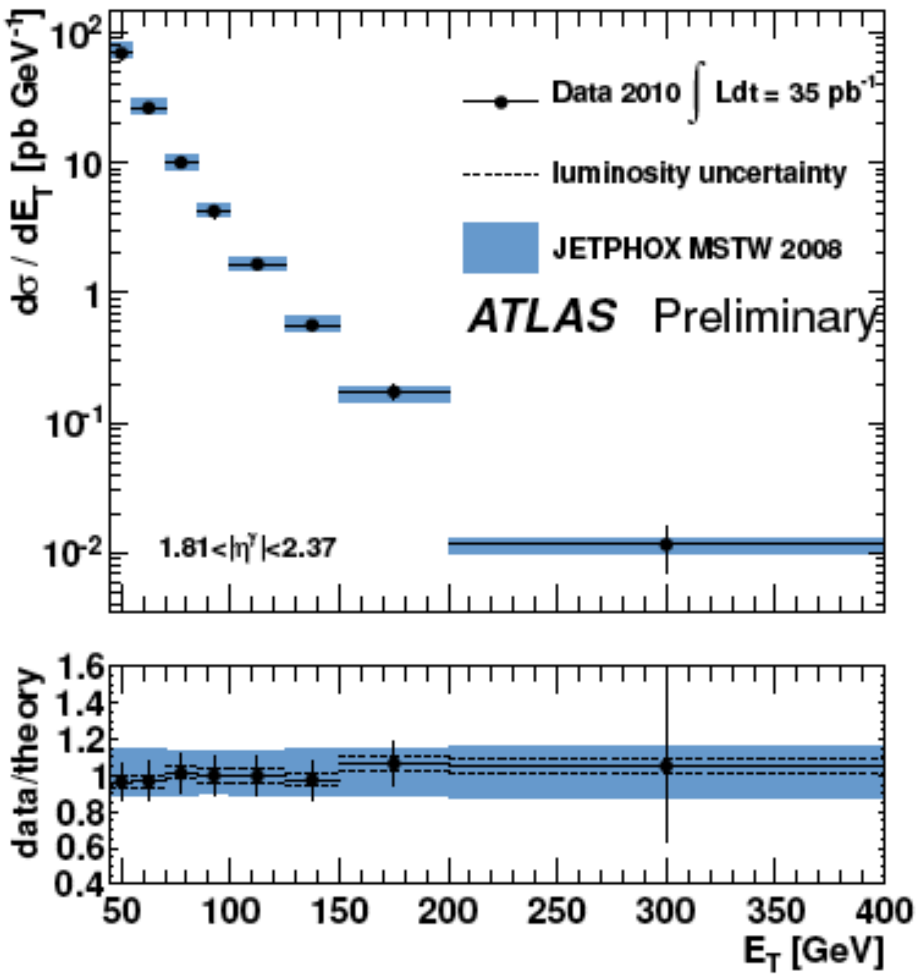

Systematics from theory:

- CTEQ 6.6 PDFs (MSTW2008: 3-5% difference) uncertainty : 4%->2%
- Fragmentation/factorization/normalization scales: 20% -> 8%
- Parton E_T^{ISO} < 4 GeV: 2%

DI-PHOTONS CROSS-SECTION MEASUREMENT @ $\sqrt{s}$ = 7 TeV

- **CERN-PH-EP-2011-08:** $L = 37\ pb^{-1}$, $E_T(\gamma) > 16$ GeV

BACKGROUND DETERMINATION: E_T^{ISO} FIT AND SIDEBANDS METHODS

FIT WITH ISOLATION TEMPLATE

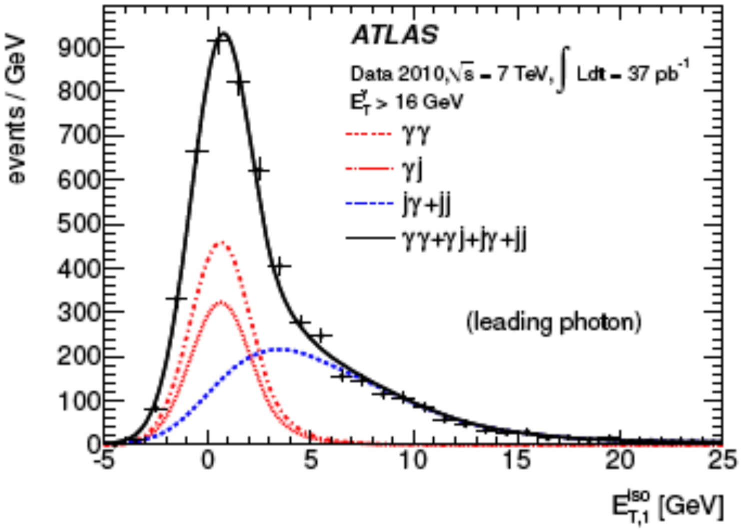

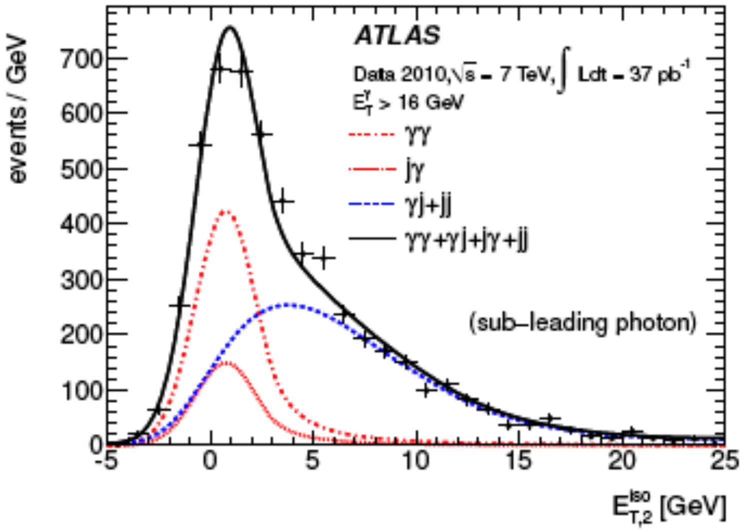

SIDEBANDS METHOD

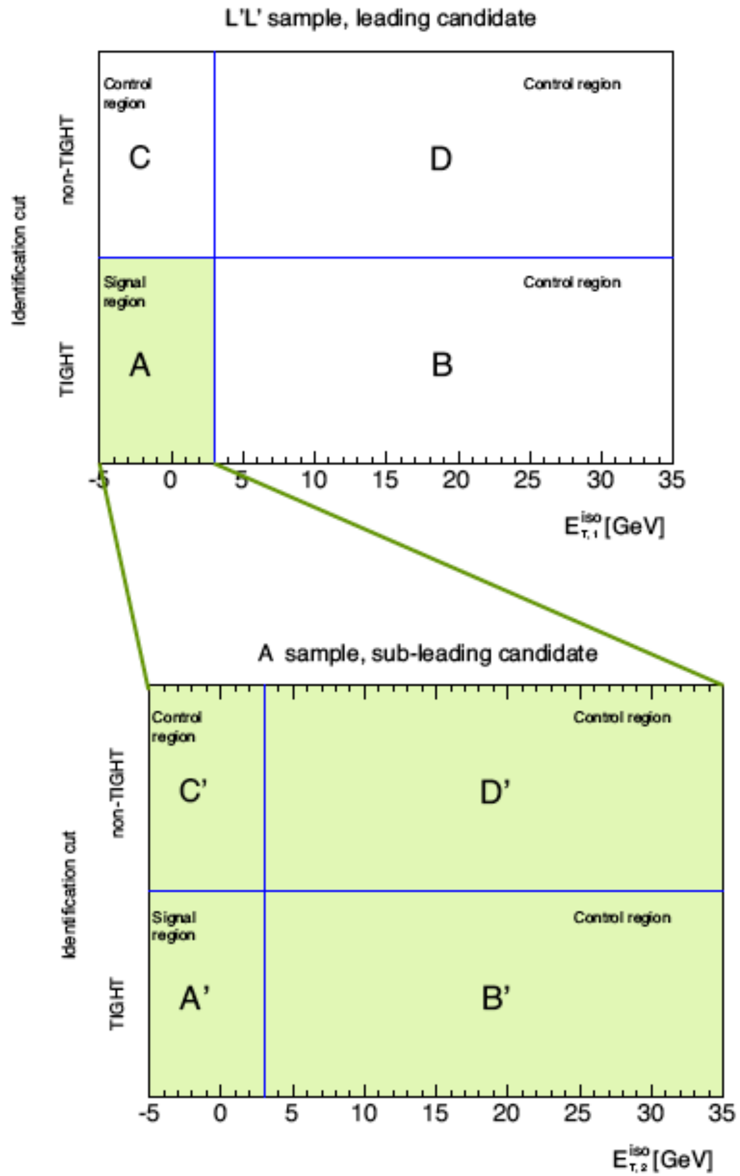

BACKGROUND DETERMINATION: EVENT WEIGHTING

$$\begin{pmatrix} \mathrm{PP} \\ \mathrm{PF} \\ \mathrm{FP} \\ \mathrm{FF} \end{pmatrix} = \begin{pmatrix} \epsilon_1\epsilon_2 & \epsilon_1 f_2 & f_1\epsilon_2 & f_1 f_2 \\ \epsilon_1(1-\epsilon_2) & \epsilon_1(1-f_2) & f_1(1-\epsilon_2) & f_1(1-f_2) \\ (1-\epsilon_1)\epsilon_2 & (1-\epsilon_1)f_2 & (1-f_1)\epsilon_2 & (1-f_1)f_2 \\ (1-\epsilon_1)(1-\epsilon_2) & (1-\epsilon_1)(1-f_2) & (1-f_1)(1-\epsilon_2) & (1-f_1)(1-f_2) \end{pmatrix} \begin{pmatrix} W_{\gamma\gamma} \\ W_{\gamma j} \\ W_{j\gamma} \\ W_{jj} \end{pmatrix}$$

P = pass E_T^{ISO} cut
F = fail E_T^{ISO} cut

- ε = probability for a γ to pass E_T^{ISO} cut (data driven)
- f = probability for a jet to pass E_T^{ISO} cut (data driven)
- Correlations in the E_T^{ISO} of the 2 γ candidates taken into account

event weights

$$N_{\gamma\gamma} = \sum \epsilon_1^{(k)} \epsilon_2^{(k)} W_{\gamma\gamma}^{(k)}$$

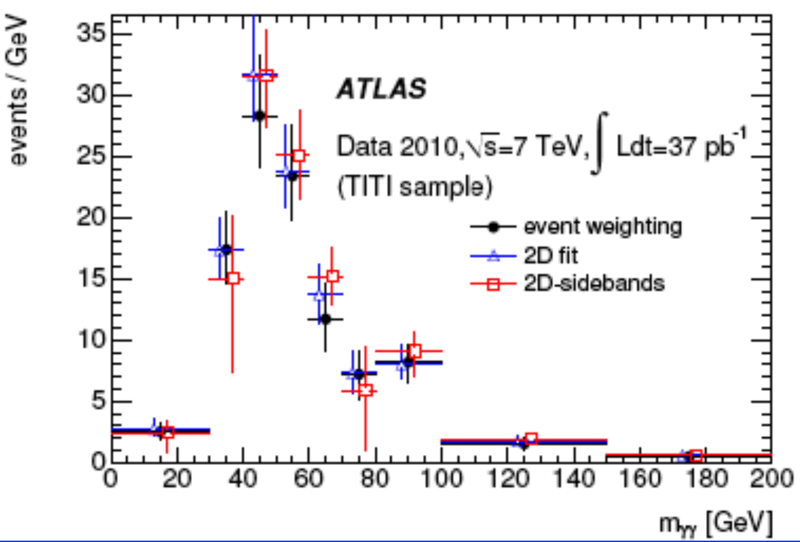

Subtract $e^{\pm}$ contribution, estimated from $\gamma e^{\pm}$ close to Z on data.

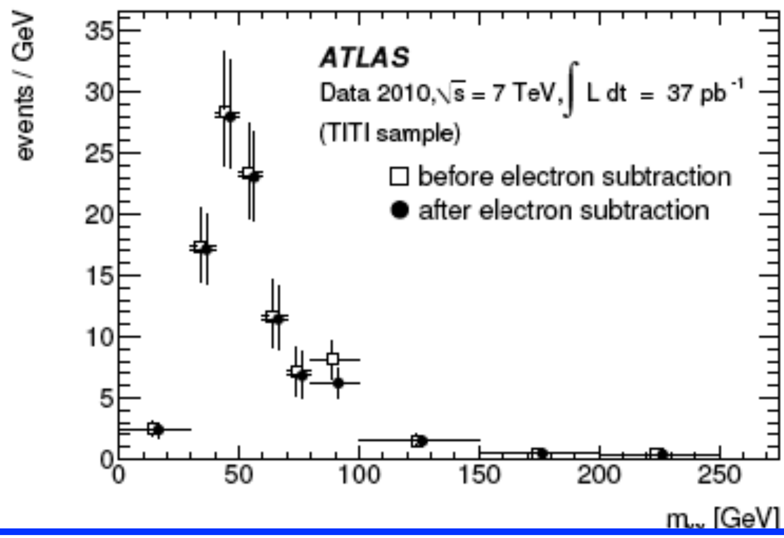

ISOLATED DI-PHOTON CROSS-SECTION 1

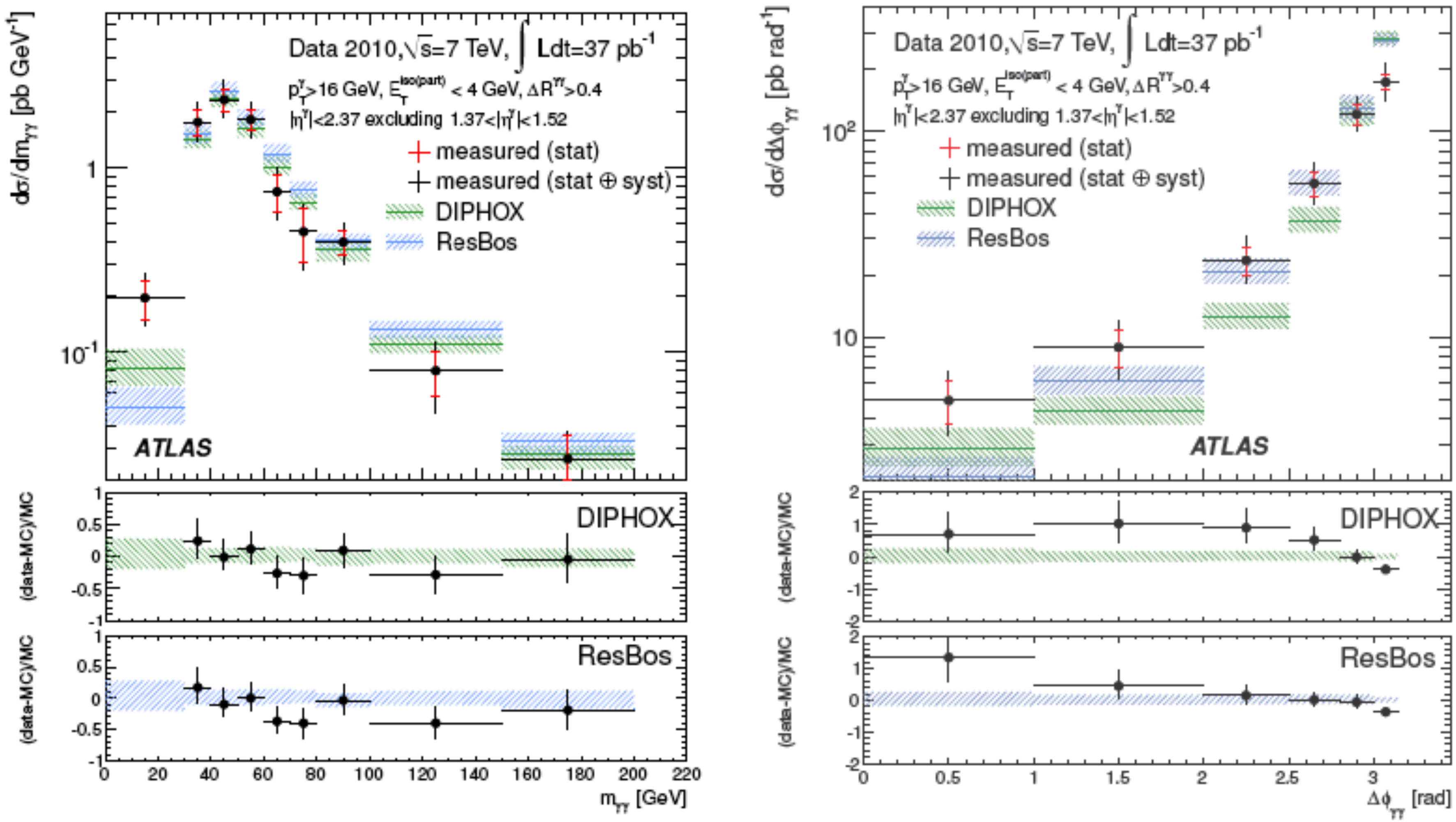

- Comparison to DIPHOX and ResBos predictions using CTEQ 6.6
- Broader distribution observed for $d\sigma/d\Delta\phi$
- Correlated to discrepancies in $d\sigma/dm_{\gamma\gamma}$ for $m_{\gamma\gamma}<2E_T$ cut

ISOLATED DIPHOTON CROSS-SECTION 2

- Experimental uncertainties:
  - energy scale: +3%, -1%
  - simulation of isolation: -7%
  - additional material: 10%
  - difference PYTHIA vs SHERPA: 5%

- Theoretical uncertainties:
  - scales variations: from $1/2m_{\gamma\gamma}$ to $2m_{\gamma\gamma}$
  - partonic isolation: 5%
  - MSTW 2008: 10% difference from CTEQ6.6

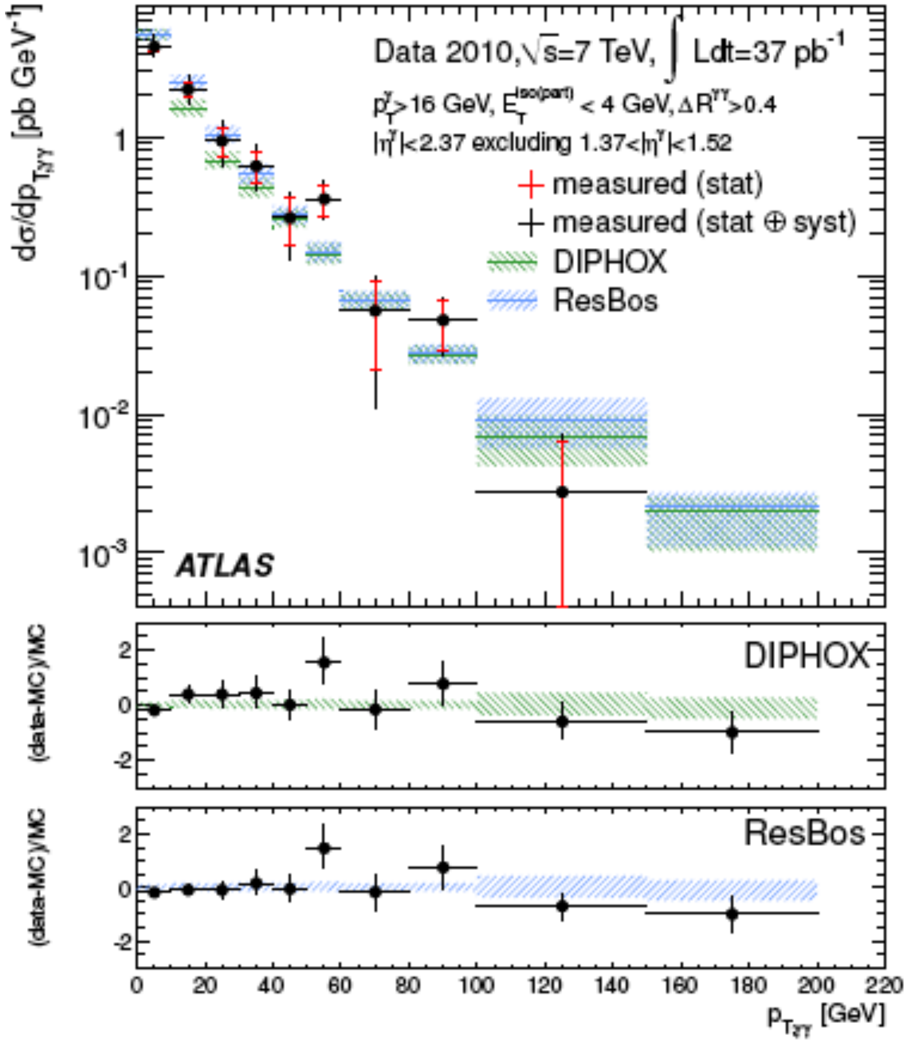

SUMMARY

- *ATLAS* measured in *pp* collisions @ √s = 7 GeV cross sections for:
  - the isolated prompt photon production;
  - the isolated di-photon production.

  SEE POSTER BY M. TRIPIANA FOR MORE DETAILS!

- The measurements profit of the good photon efficiency (85% reconstruction, 95% identification) and of the high purity (>95% above 100 GeV) achieved.

- The isolated prompt photon cross-section is:
  - well in agreement with the NLO pQCD calculations for E_T >35GeV;
  - shows some discrepancy for Et<35GeV.

- The isolated di-photon cross section measured shows some disagreement for the azimuth separation of the two photons.

- Beyond NLO calculations and a better theoretical description of the fragmentation are needed to understand the differences.

- In the meanwhile ATLAS is analysing the whole 2011 dataset to provide updated measurements and to extend the energy range explored.

INCLUSIVE PHOTON E_T SPECTRUM WITH 1.08 fb^{-1}

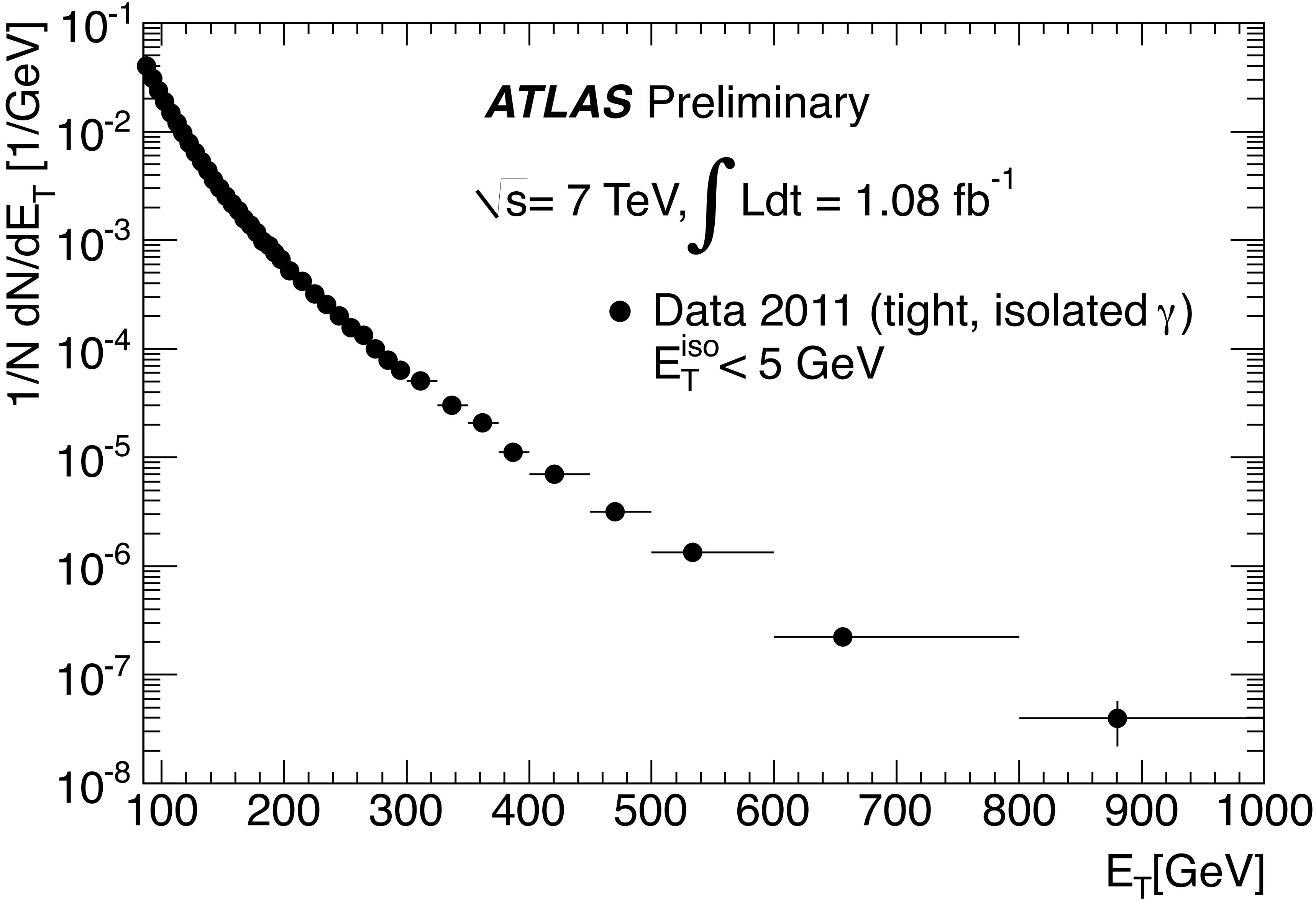

HIGHEST E_T (960 GeV) PHOTON CANDIDATE

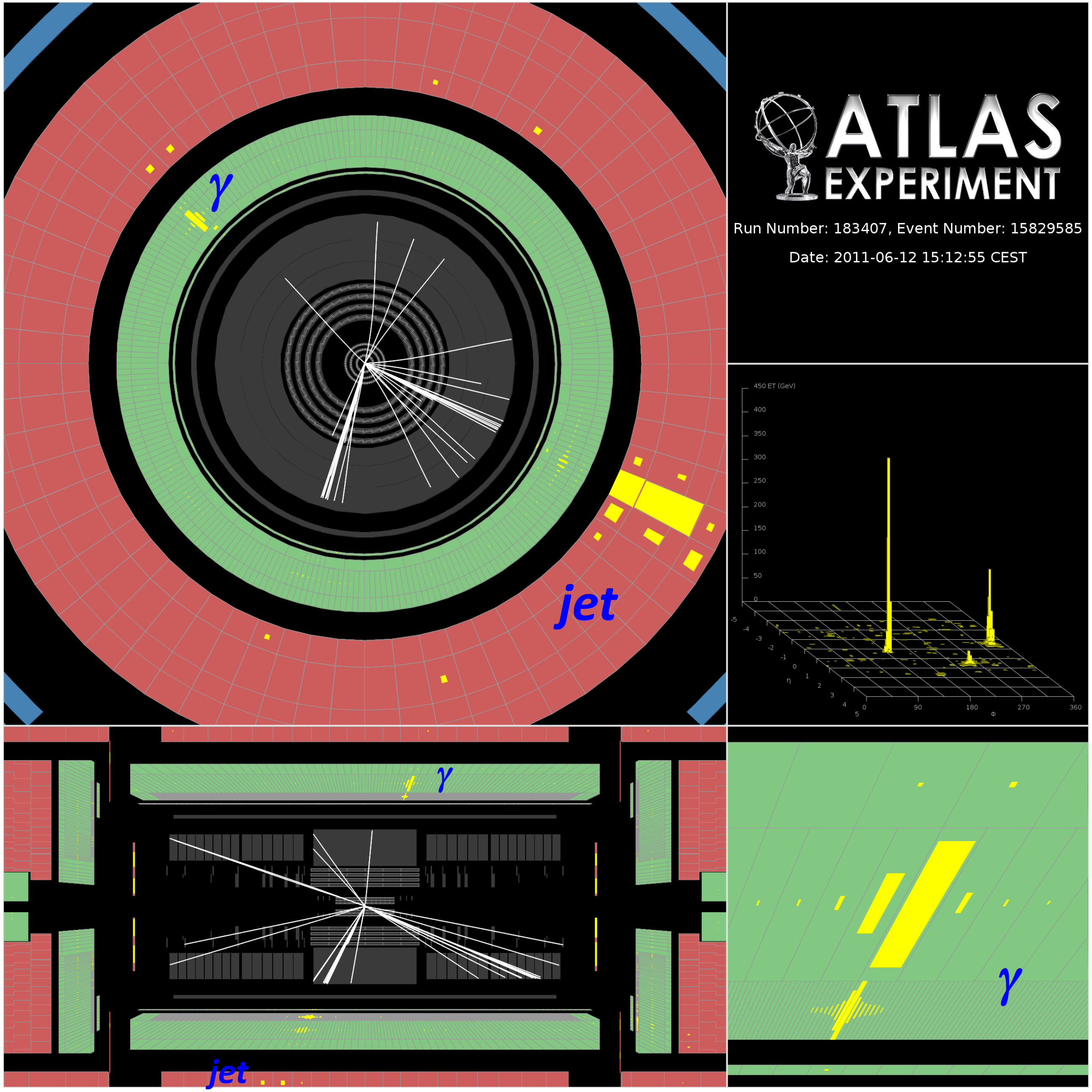

BACKUP

ISOLATION ENERGY

Use electrons from W, Z

Study e/γ differences on MC, apply to collision data.

— : from electron extrapolation

• : from non-TIGHT subtraction

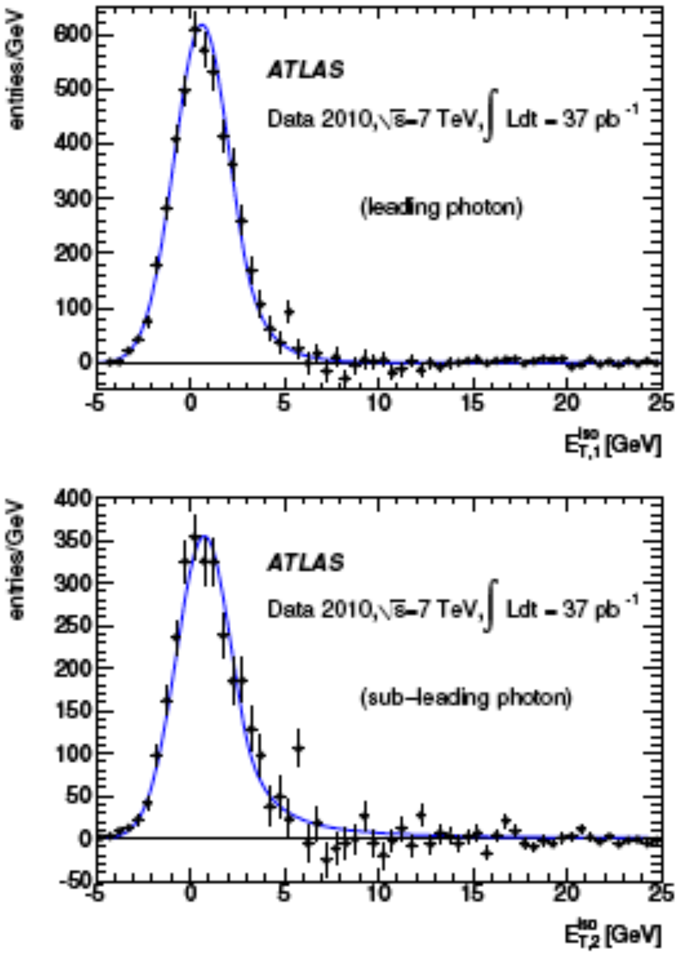

TRIGGER AND RECONSTRUCTION EFFICIENCIES

- ε_{trig} (from data): plateau at ~100% for photons passing offline selection

10 GeV threshold

$\varepsilon_{trig} = (99.5\pm0.5)\%$

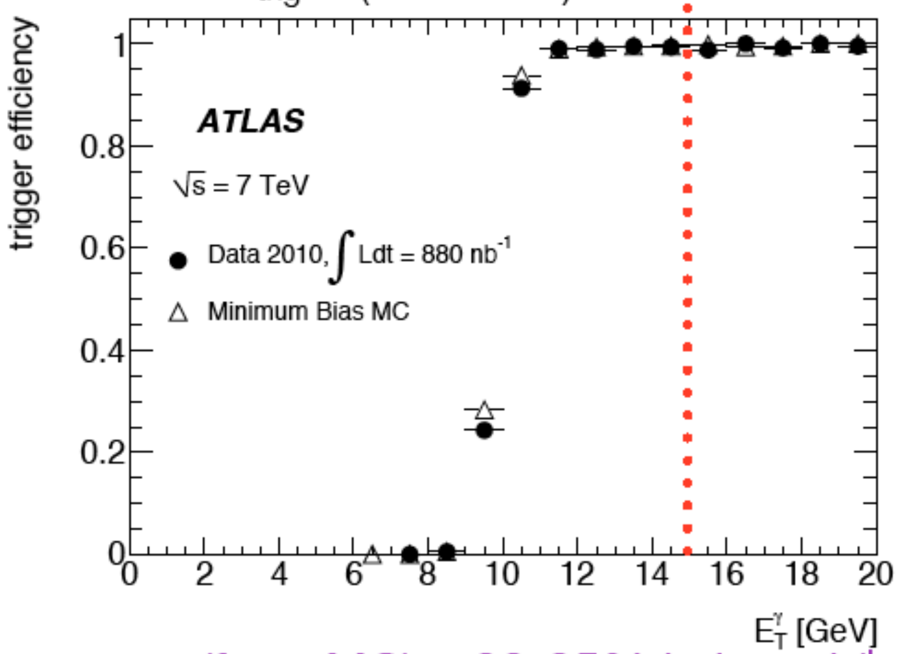

40 GeV threshold

$\varepsilon_{trig} = (99.4^{+0.6}_{-0.2})\%$

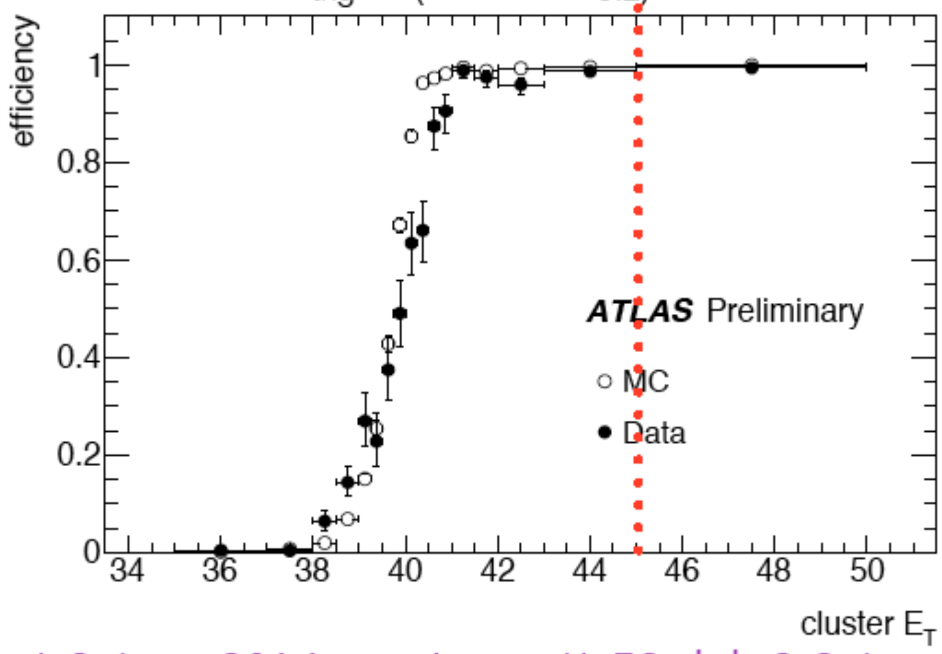

- ε_{reco} (from MC): ~80-85% in barrel ($|\eta|<1.37$), ~70% in end-cap ($1.52<|\eta|<2.37$)
  - significant part of inefficiency (dead readout) recovered in 2011 winter shutdown
  - uncertainties: extra material not in MC (1-2%), generator and fraction of fragmentation photons (<2%), experimental isolation efficiency (3-4%)

PHOTON DETECTION WITH ATLAS

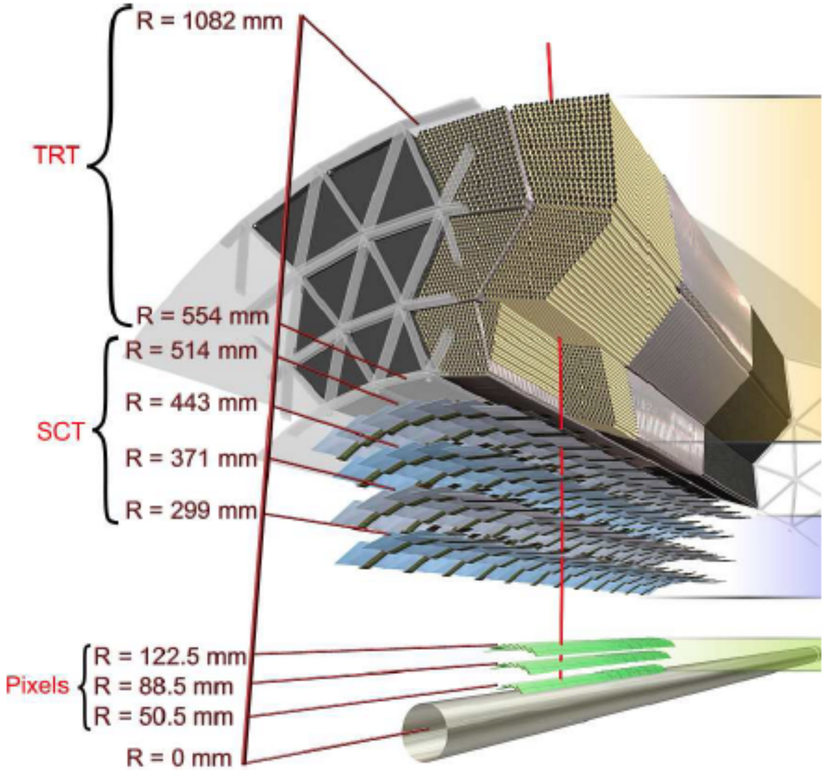

- Inner Detector ($|\eta|<2.5$)
  - track charged particles
  - measure transition radiation
  - ✓ reconstruct γ conversions
  - ✓ e/γ discrimination

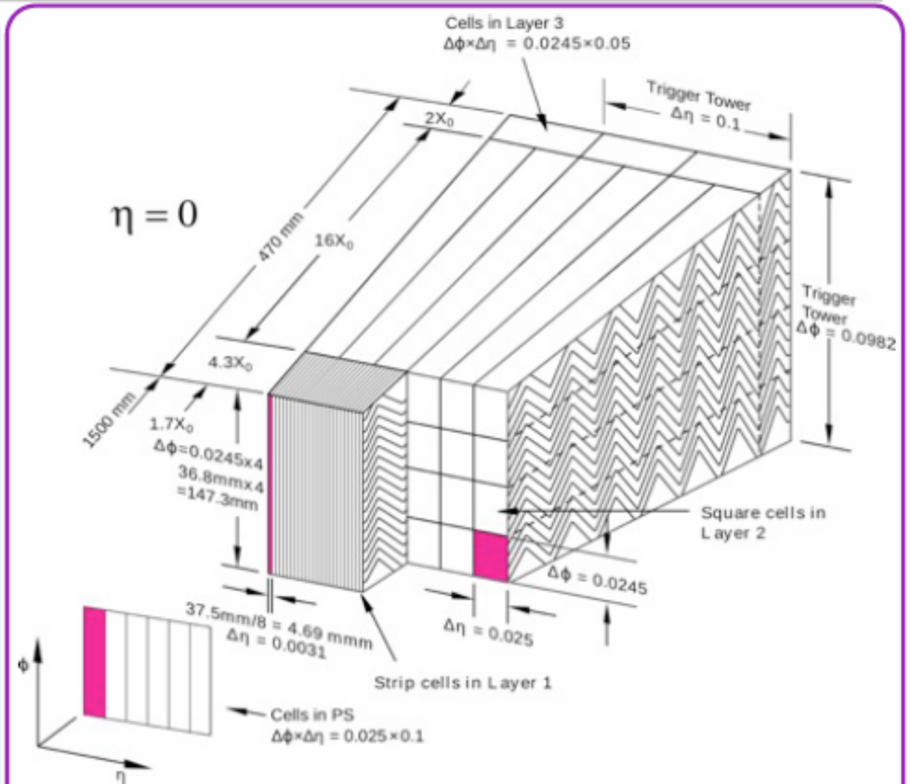

- Pb-LAr EM calorimeter
  - very fine layer 1 segmentation up to $|\eta|$=2.37
  - ✓ γ energy/direction measurement
  - ✓ π^0/γ discrimination (shower shape)

Ambient transverse energy density

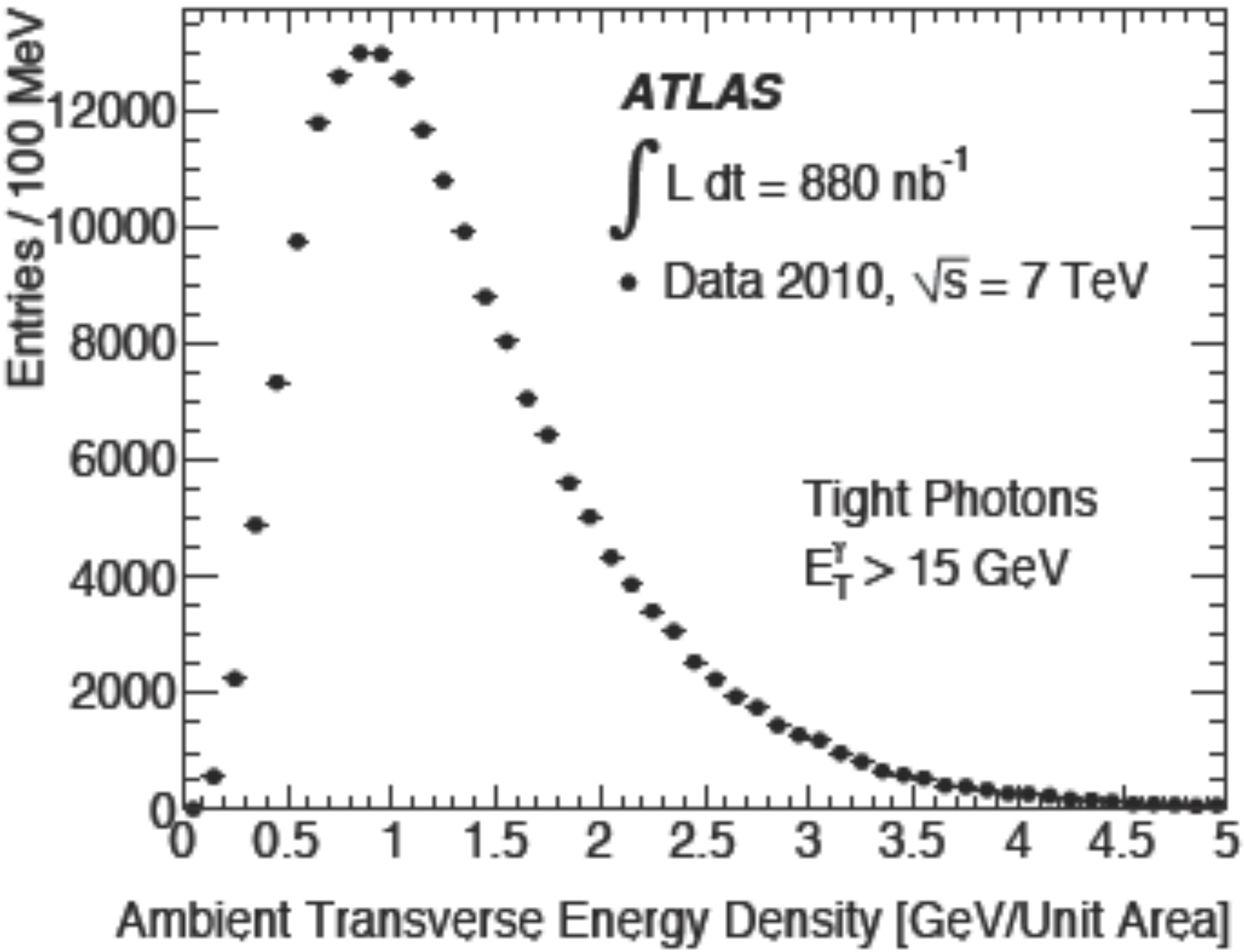

PHOTON OFFLINE SELECTION EFFICIENCY (15-100 GeV, 0.85pb^{-1})

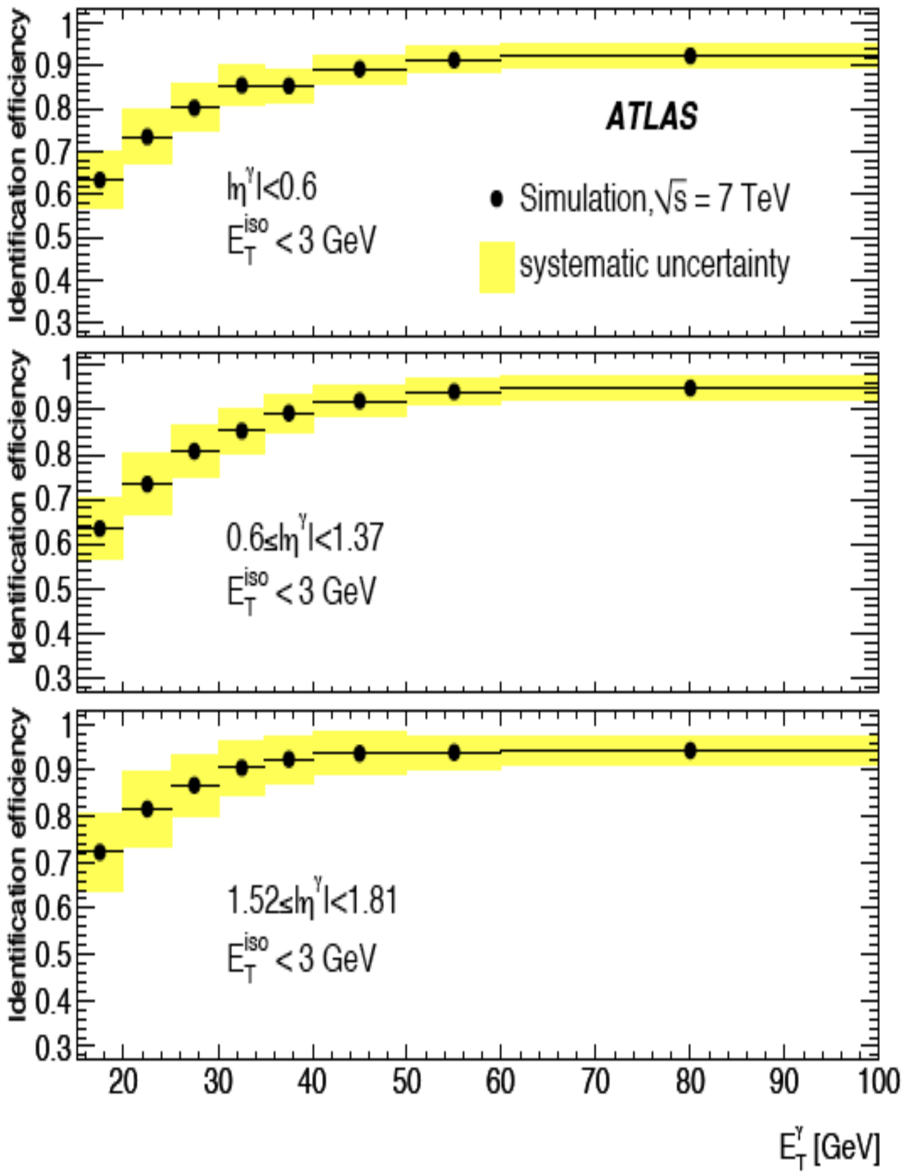

PHOTON OFFLINE SELECTION EFFICIENCY (45-400 GeV, 35pb^{-1})

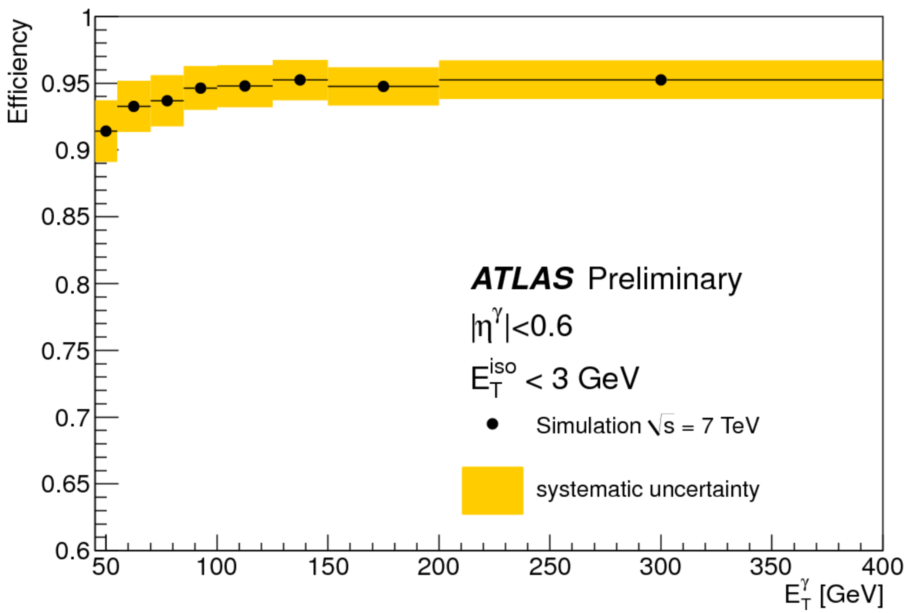

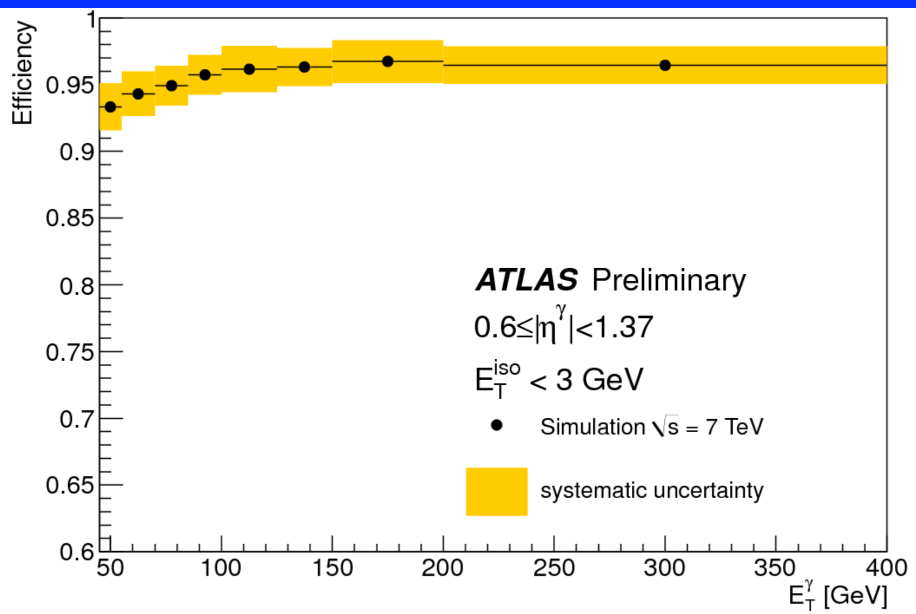

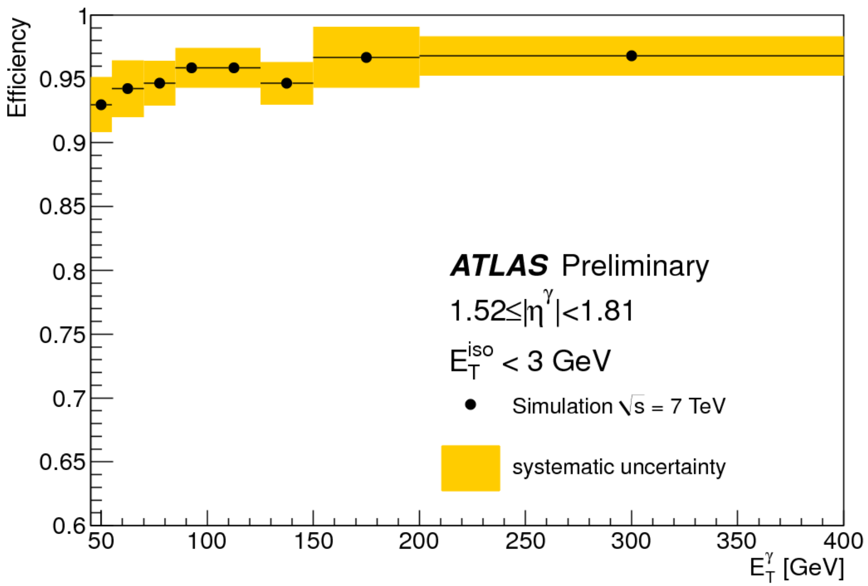

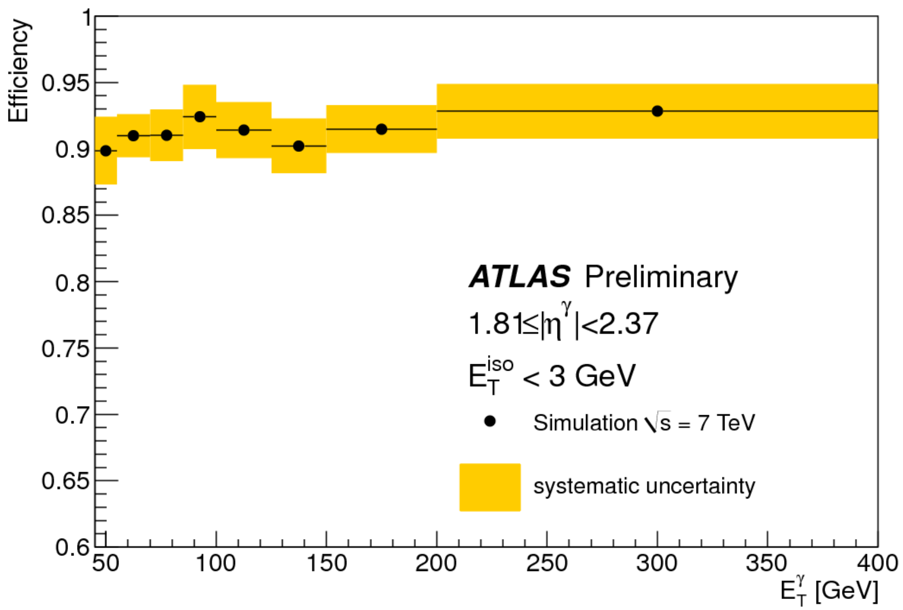

PHOTONS PURITY (15-100 GeV, 0.85pb^{-1})

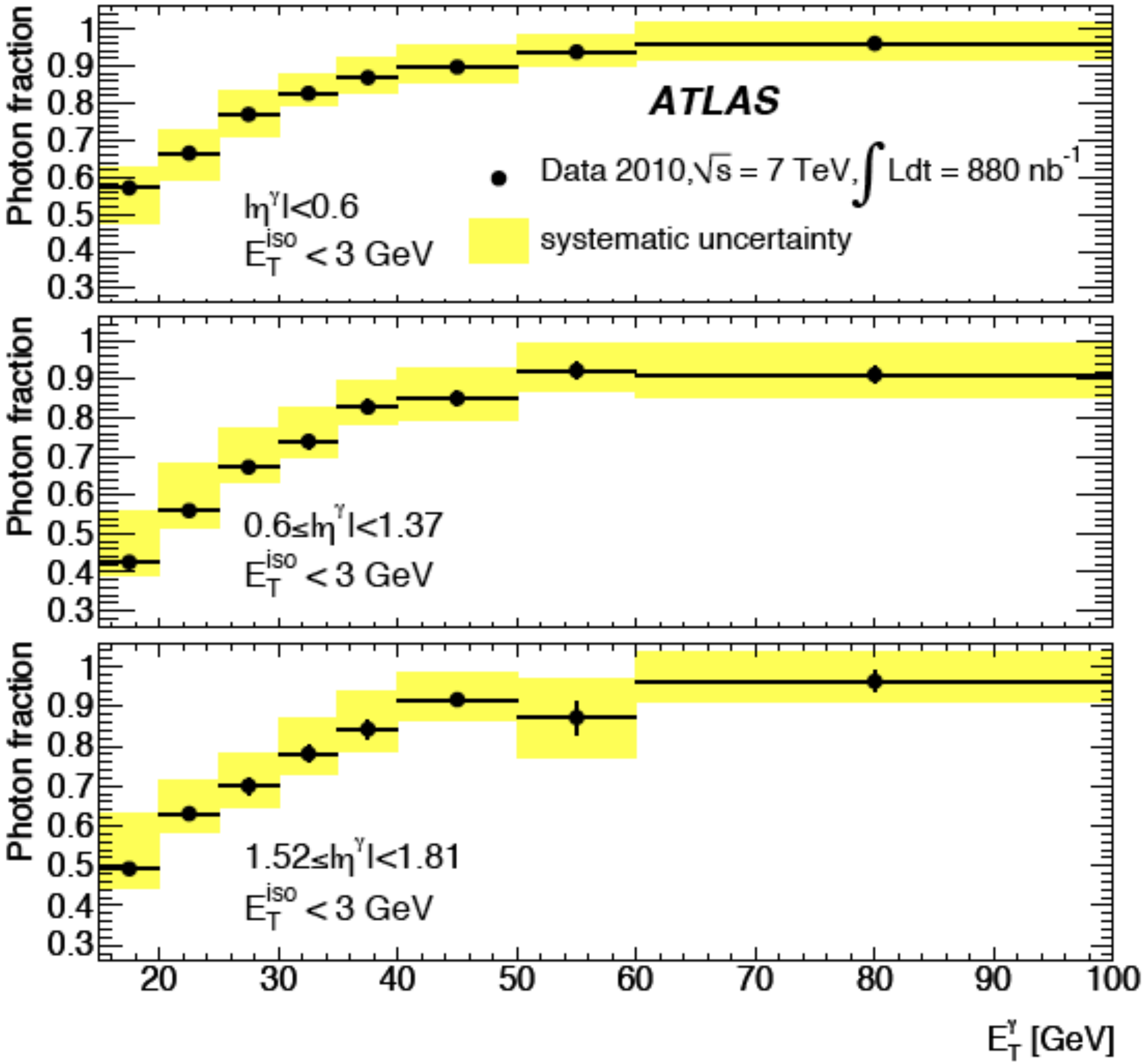

PHOTONS PURITY (45-400 GeV, 35pb^{-1})

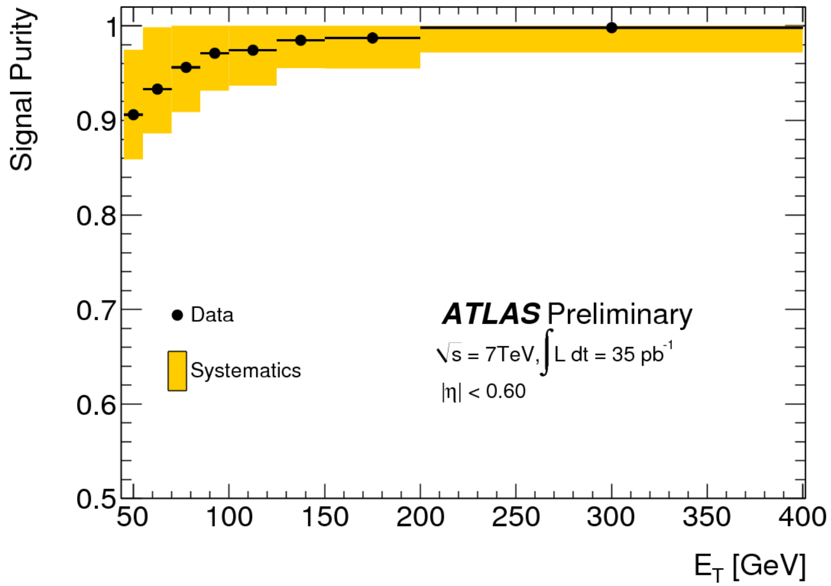

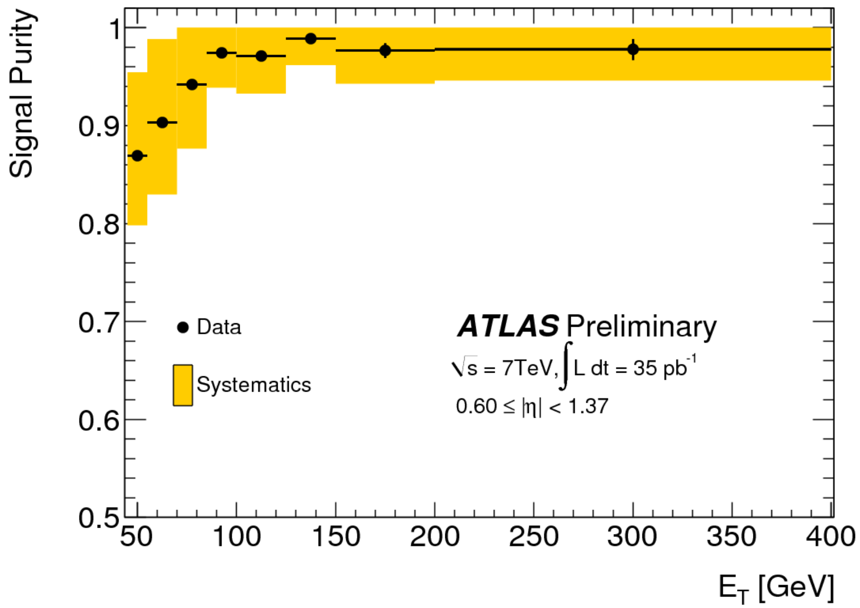

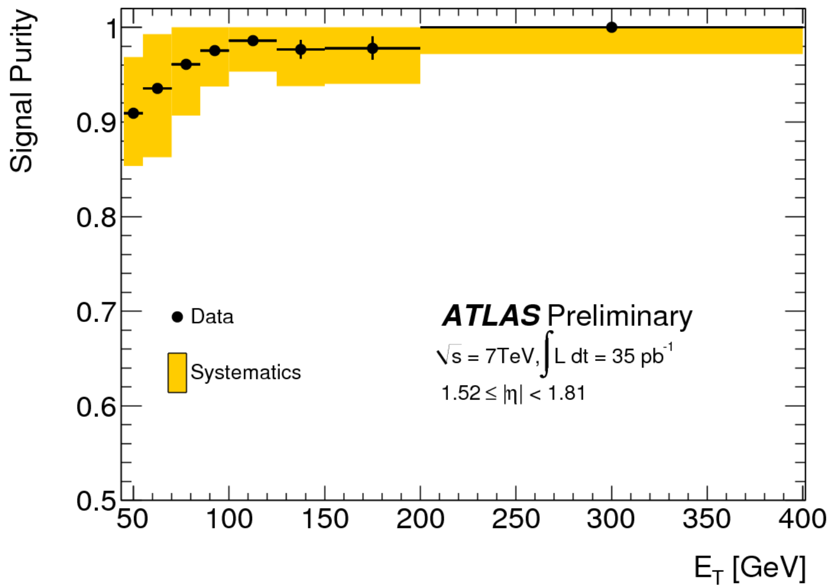

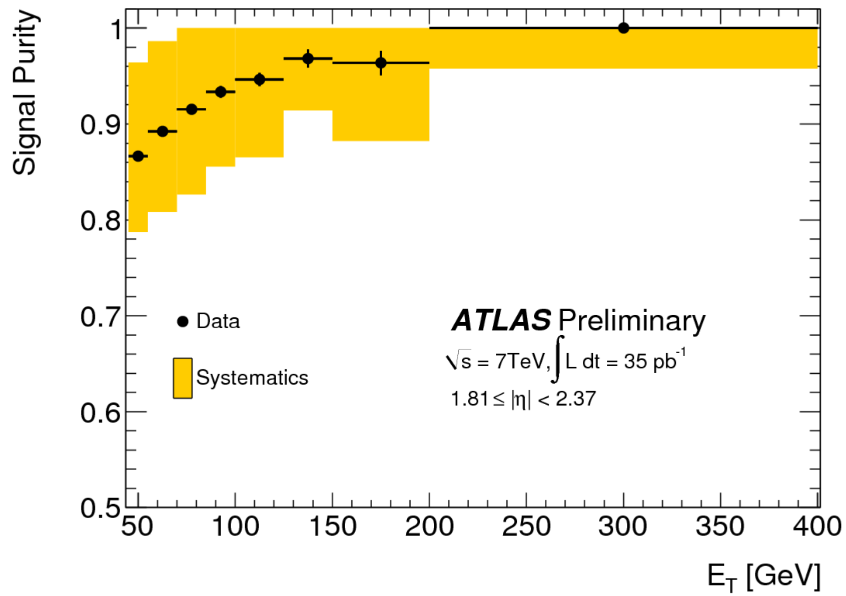

PHOTON YIELDS

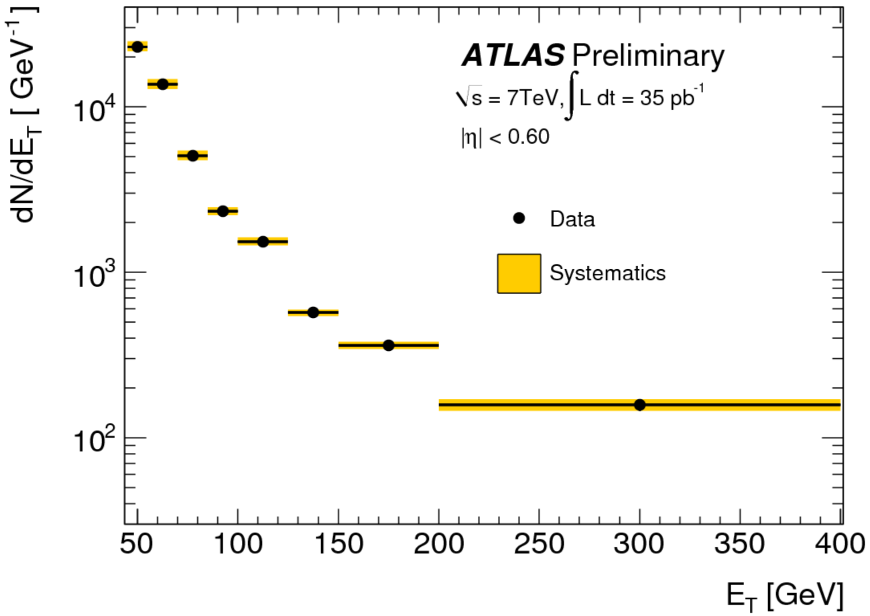

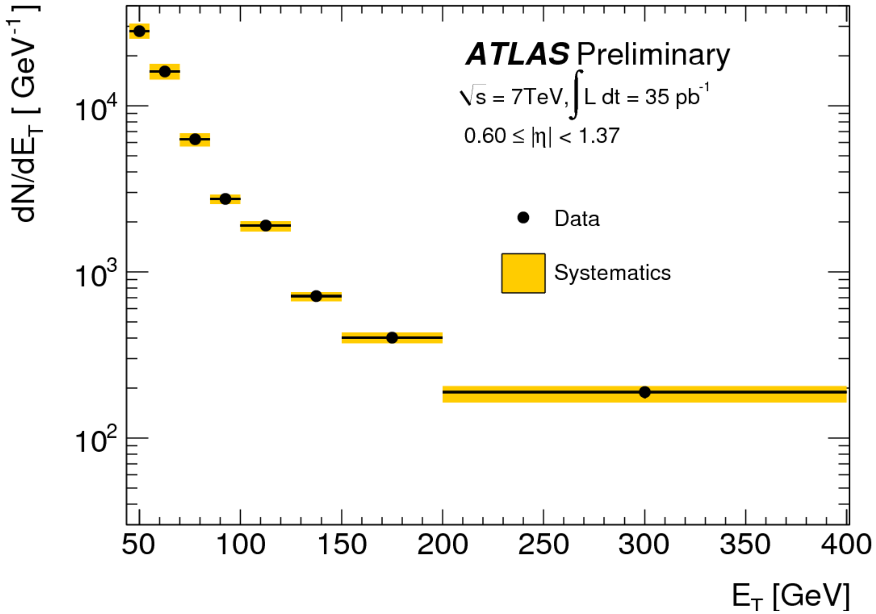

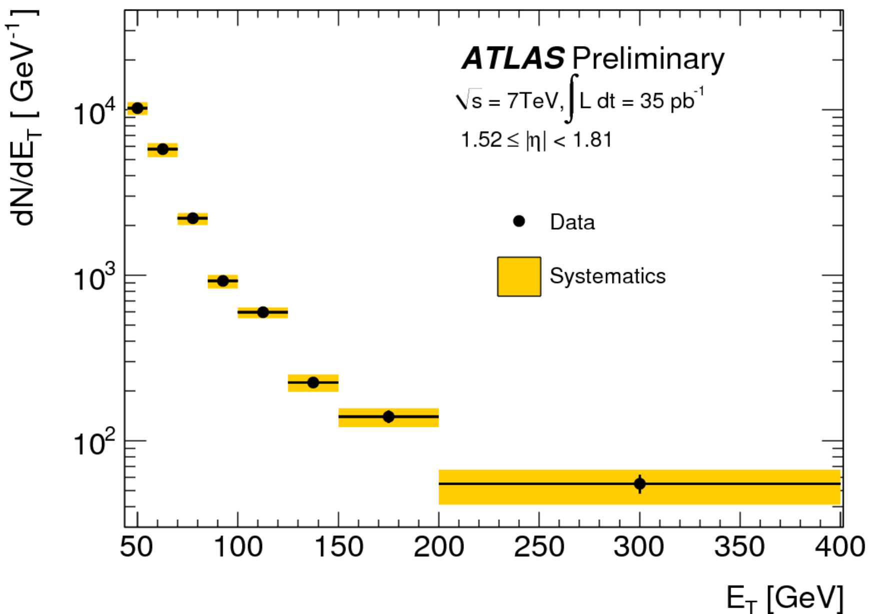

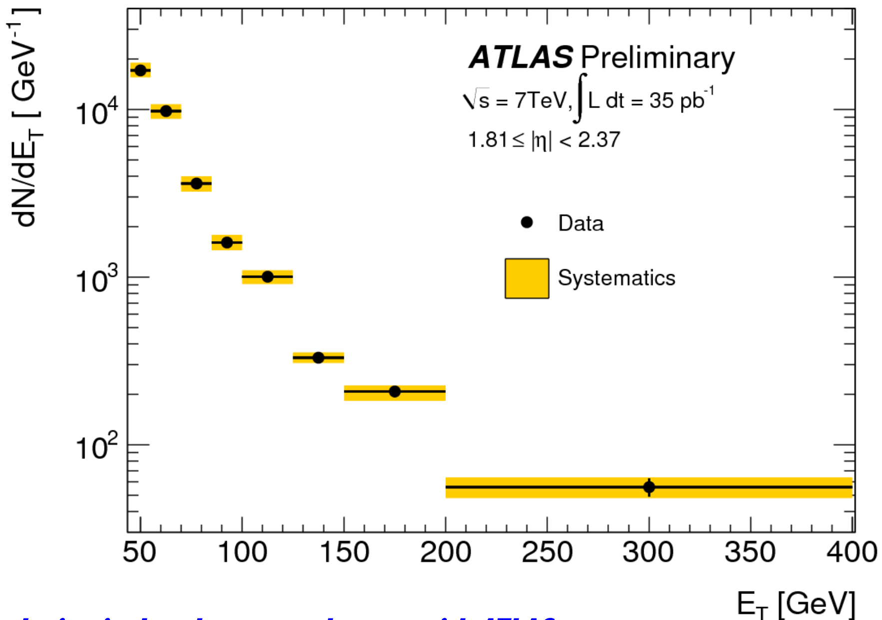

DIAGRAMS

SINGLE PHOTON

Leading processes

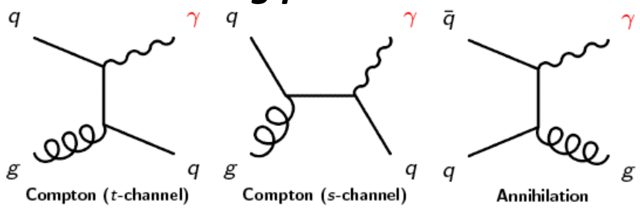

Higher Order

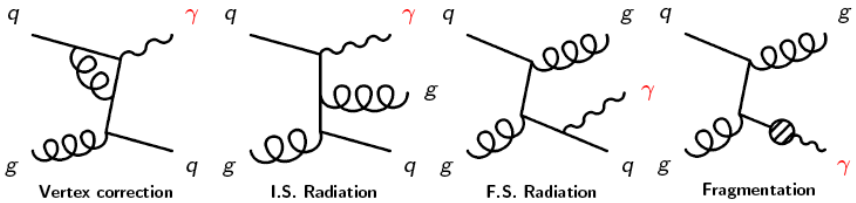

- Compton dominant respect to the annihilation
- Fragmentation, giving photons closer to hadrons, important at low E_T

DI-PHOTONS

Leading processes

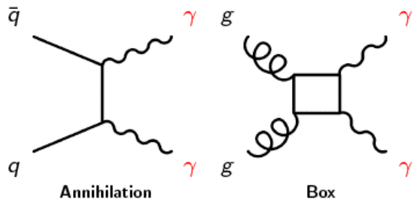

Higher Order

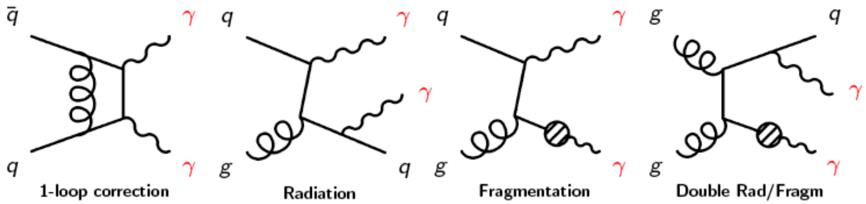

- Annihilation and box comparable due to high flux of gluons at LHC

SINGLE PHOTON CROSS-SECTION SYSTEMATICS

Systematic	Reco. Eff.	ID Eff.	Yield	Unfolding	Theory
Finite Statistics per bin				< 2%	
Generator	1%	< 1%	~ 1%	3%	
E_T Resolution				< 1%	
Photon ID			< 5%		
Photon Isolation			< 1%		
Signal Leakage			2% – 8%		
Background Correlations			< 4%		
Energy Scale			2% – 8%		
Material	1% – 4%	1% – 2%	< 1%		
Soft-jet Energy Density			3% – 7%		
Transverse Energy Leakage			1% – 4%		
Hard/Brem Composition	1%	< 1%	1% – 7%		
OTX	0.2%				
Photon Isolation Cut	3% – 4%				
Intrinsic Precision		1% – 3%			
Photon Sample Selection		0.5%			
Conv/Unconv. Photon Ratio		< 1%			
Scale uncertainty					10% – 20%
PDFs					2% – 5%
Parton level Isolation					< 2%

DI-PHOTONS CROSS-SECTION SYSTEMATICS

$m_{\gamma\gamma}$ [GeV]	$\tilde{\mathrm{T}}$	$\tilde{\mathrm{I}}$	matrix	$e \to \gamma$	ID	material	generator	σ_E	E-scale	$E_{\mathrm{T}}^{\mathrm{iso(part)}}$	$\int Ldt$
0 – 30	$^{+0.03}_{-0.01}$	$^{+0.000}_{-0.005}$	$^{+0.021}_{-0.022}$	$^{+0.002}_{-0.002}$	$^{+0.020}_{-0.017}$	$^{+0.021}_{-0.000}$	$^{+0.03}_{-0.00}$	$^{+0.001}_{-0.000}$	$^{+0.006}_{-0.002}$	$^{+0.000}_{-0.010}$	$^{+0.007}_{-0.007}$
30 – 40	$^{+0.17}_{-0.09}$	$^{+0.00}_{-0.05}$	$^{+0.13}_{-0.13}$	$^{+0.008}_{-0.008}$	$^{+0.22}_{-0.18}$	$^{+0.3}_{-0.0}$	$^{+0.014}_{-0.000}$	$^{+0.003}_{-0.000}$	$^{+0.04}_{-0.03}$	$^{+0.00}_{-0.09}$	$^{+0.06}_{-0.06}$
40 – 50	$^{+0.3}_{-0.1}$	$^{+0.00}_{-0.06}$	$^{+0.19}_{-0.19}$	$^{+0.008}_{-0.008}$	$^{+0.24}_{-0.20}$	$^{+0.3}_{-0.0}$	$^{+0.11}_{-0.00}$	$^{+0.024}_{-0.000}$	$^{+0.09}_{-0.03}$	$^{+0.00}_{-0.17}$	$^{+0.08}_{-0.08}$
50 – 60	$^{+0.20}_{-0.13}$	$^{+0.00}_{-0.04}$	$^{+0.14}_{-0.14}$	$^{+0.007}_{-0.007}$	$^{+0.15}_{-0.13}$	$^{+0.19}_{-0.00}$	$^{+0.05}_{-0.00}$	$^{+0.003}_{-0.000}$	$^{+0.06}_{-0.03}$	$^{+0.00}_{-0.13}$	$^{+0.06}_{-0.06}$
60 – 70	$^{+0.14}_{-0.06}$	$^{+0.001}_{-0.016}$	$^{+0.09}_{-0.09}$	$^{+0.004}_{-0.004}$	$^{+0.05}_{-0.04}$	$^{+0.07}_{-0.00}$	$^{+0.04}_{-0.00}$	$^{+0.007}_{-0.000}$	$^{+0.03}_{-0.02}$	$^{+0.00}_{-0.05}$	$^{+0.03}_{-0.03}$
70 – 80	$^{+0.06}_{-0.06}$	$^{+0.000}_{-0.007}$	$^{+0.05}_{-0.06}$	$^{+0.003}_{-0.003}$	$^{+0.03}_{-0.03}$	$^{+0.07}_{-0.00}$	$^{+0.03}_{-0.00}$	$^{+0.002}_{-0.001}$	$^{+0.009}_{-0.002}$	$^{+0.00}_{-0.03}$	$^{+0.015}_{-0.015}$
80 – 100	$^{+0.04}_{-0.05}$	$^{+0.000}_{-0.005}$	$^{+0.04}_{-0.04}$	$^{+0.019}_{-0.019}$	$^{+0.03}_{-0.02}$	$^{+0.04}_{-0.00}$	$^{+0.012}_{-0.000}$	$^{+0.004}_{-0.000}$	$^{+0.013}_{-0.003}$	$^{+0.00}_{-0.03}$	$^{+0.013}_{-0.013}$
100 – 150	$^{+0.019}_{-0.016}$	$^{+0.001}_{-0.001}$	$^{+0.015}_{-0.018}$	$^{+0.001}_{-0.001}$	$^{+0.004}_{-0.003}$	$^{+0.002}_{-0.001}$	$^{+0.004}_{-0.000}$	$^{+0.000}_{-0.001}$	$^{+0.002}_{-0.003}$	$^{+0.000}_{-0.005}$	$^{+0.003}_{-0.003}$
150 – 200	$^{+0.002}_{-0.002}$	$^{+0.000}_{-0.000}$	$^{+0.003}_{-0.003}$	$^{+0.000}_{-0.000}$	$^{+0.002}_{-0.001}$	$^{+0.004}_{-0.000}$	$^{+0.001}_{-0.000}$	$^{+0.000}_{-0.000}$	$^{+0.001}_{-0.000}$	$^{+0.000}_{-0.002}$	$^{+0.001}_{-0.001}$

DI-PHOTONS CROSS-SECTION SYSTEMATICS

$p_{T,\gamma\gamma}$ [GeV]	$\tilde{\mathbf{T}}$	$\tilde{\mathbf{I}}$	matrix	$e \to \gamma$	ID	material	generator	σ_E	E-scale	$E_T^{\mathrm{iso(part)}}$	$\int L dt$
0 – 10	$^{+0.3}_{-0.2}$	$^{+0.00}_{-0.09}$	$^{+0.3}_{-0.3}$	$^{+0.03}_{-0.03}$	$^{+0.4}_{-0.4}$	$^{+0.6}_{-0.0}$	$^{+0.10}_{-0.00}$	$^{+0.03}_{-0.00}$	$^{+0.12}_{-0.05}$	$^{+0.0}_{-0.3}$	$^{+0.15}_{-0.15}$
10 – 20	$^{+0.3}_{-0.2}$	$^{+0.00}_{-0.05}$	$^{+0.21}_{-0.22}$	$^{+0.015}_{-0.015}$	$^{+0.20}_{-0.17}$	$^{+0.21}_{-0.00}$	$^{+0.11}_{-0.00}$	$^{+0.001}_{-0.001}$	$^{+0.06}_{-0.03}$	$^{+0.00}_{-0.15}$	$^{+0.08}_{-0.08}$
20 – 30	$^{+0.21}_{-0.16}$	$^{+0.000}_{-0.025}$	$^{+0.13}_{-0.14}$	$^{+0.008}_{-0.008}$	$^{+0.07}_{-0.06}$	$^{+0.10}_{-0.00}$	$^{+0.022}_{-0.000}$	$^{+0.010}_{-0.000}$	$^{+0.03}_{-0.02}$	$^{+0.00}_{-0.08}$	$^{+0.03}_{-0.03}$
30 – 40	$^{+0.13}_{-0.08}$	$^{+0.000}_{-0.012}$	$^{+0.09}_{-0.10}$	$^{+0.006}_{-0.006}$	$^{+0.06}_{-0.05}$	$^{+0.11}_{-0.00}$	$^{+0.08}_{-0.00}$	$^{+0.007}_{-0.000}$	$^{+0.015}_{-0.009}$	$^{+0.00}_{-0.03}$	$^{+0.021}_{-0.021}$
40 – 50	$^{+0.08}_{-0.06}$	$^{+0.000}_{-0.007}$	$^{+0.05}_{-0.06}$	$^{+0.004}_{-0.004}$	$^{+0.018}_{-0.017}$	$^{+0.03}_{-0.00}$	$^{+0.005}_{-0.000}$	$^{+0.000}_{-0.012}$	$^{+0.00}_{-0.03}$	$^{+0.000}_{-0.015}$	$^{+0.009}_{-0.009}$
50 – 60	$^{+0.03}_{-0.03}$	$^{+0.000}_{-0.007}$	$^{+0.02}_{-0.03}$	$^{+0.006}_{-0.006}$	$^{+0.03}_{-0.02}$	$^{+0.04}_{-0.00}$	$^{+0.04}_{-0.00}$	$^{+0.013}_{-0.000}$	$^{+0.05}_{-0.01}$	$^{+0.000}_{-0.023}$	$^{+0.012}_{-0.012}$
60 – 80	$^{+0.021}_{-0.023}$	$^{+0.000}_{-0.001}$	$^{+0.014}_{-0.016}$	$^{+0.001}_{-0.001}$	$^{+0.003}_{-0.003}$	$^{+0.005}_{-0.000}$	$^{+0.000}_{-0.004}$	$^{+0.000}_{-0.001}$	$^{+0.000}_{-0.002}$	$^{+0.000}_{-0.004}$	$^{+0.002}_{-0.002}$
80 – 100	$^{+0.006}_{-0.000}$	$^{+0.000}_{-0.001}$	$^{+0.005}_{-0.005}$	$^{+0.002}_{-0.002}$	$^{+0.003}_{-0.002}$	$^{+0.002}_{-0.006}$	$^{+0.000}_{-0.005}$	$^{+0.001}_{-0.000}$	$^{+0.004}_{-0.001}$	$^{+0.000}_{-0.004}$	$^{+0.002}_{-0.002}$
100 – 150	$^{+0.002}_{-0.001}$	$^{+0.000}_{-0.000}$	$^{+0.001}_{-0.002}$	$^{+0.000}_{-0.000}$	$^{+0.000}_{-0.000}$	$^{+0.000}_{-0.000}$	$^{+0.000}_{-0.001}$	$^{+0.000}_{-0.000}$	$^{+0.000}_{-0.000}$	$^{+0.000}_{-0.000}$	$^{+0.000}_{-0.000}$
150 – 200	$^{+0.000}_{-0.000}$	$^{+0.000}_{-0.000}$	$^{+0.000}_{-0.000}$	$^{+0.000}_{-0.000}$	$^{+0.000}_{-0.000}$	$^{+0.000}_{-0.000}$	$^{+0.000}_{-0.000}$	$^{+0.000}_{-0.000}$	$^{+0.000}_{-0.000}$	$^{+0.000}_{-0.000}$	$^{+0.000}_{-0.000}$

$\Delta\phi_{\gamma\gamma}$ [rad]	$\tilde{\mathbf{T}}$	$\tilde{\mathbf{I}}$	matrix	$e \to \gamma$	ID	material	generator	σ_E	E-scale	$E_T^{\mathrm{iso(part)}}$	$\int L dt$
0.00 – 1.00	$^{+1.1}_{-0.5}$	$^{+0.00}_{-0.14}$	$^{+0.8}_{-0.8}$	$^{+0.05}_{-0.05}$	$^{+0.4}_{-0.4}$	$^{+0.4}_{-0.0}$	$^{+0.3}_{-0.0}$	$^{+0.000}_{-0.017}$	$^{+0.14}_{-0.08}$	$^{+0.0}_{-0.3}$	$^{+0.17}_{-0.17}$
1.00 – 2.00	$^{+1.6}_{-1.0}$	$^{+0.0}_{-0.3}$	$^{+1.2}_{-1.2}$	$^{+0.07}_{-0.07}$	$^{+0.8}_{-0.7}$	$^{+1.0}_{-0.0}$	$^{+0.5}_{-0.0}$	$^{+0.023}_{-0.000}$	$^{+0.23}_{-0.10}$	$^{+0.0}_{-0.5}$	$^{+0.3}_{-0.3}$
2.00 – 2.50	$^{+3}_{-2}$	$^{+0.0}_{-0.4}$	$^{+2.2}_{-2.3}$	$^{+0.17}_{-0.17}$	$^{+2.2}_{-1.8}$	$^{+3}_{-0}$	$^{+1.5}_{-0.0}$	$^{+0.10}_{-0.00}$	$^{+0.6}_{-0.4}$	$^{+0.0}_{-1.3}$	$^{+0.8}_{-0.8}$
2.50 – 2.80	$^{+6}_{-5}$	$^{+0.0}_{-1.3}$	$^{+5}_{-5}$	$^{+0.4}_{-0.4}$	$^{+5}_{-4}$	$^{+6}_{-0}$	$^{+0.3}_{-0.0}$	$^{+0.4}_{-0.0}$	$^{+1.8}_{-1.0}$	$^{+0}_{-4}$	$^{+1.9}_{-1.9}$
2.80 – 3.00	$^{+11}_{-5}$	$^{+0}_{-3}$	$^{+9}_{-10}$	$^{+0.9}_{-0.9}$	$^{+11}_{-9}$	$^{+14}_{-0}$	$^{+2.3}_{-0.0}$	$^{+0.7}_{-0.0}$	$^{+4}_{-1}$	$^{+0}_{-9}$	$^{+4}_{-4}$
3.00 – 3.14	$^{+19}_{-16}$	$^{+0}_{-3}$	$^{+14}_{-15}$	$^{+1.5}_{-1.5}$	$^{+16}_{-13}$	$^{+18}_{-0}$	$^{+9}_{-0}$	$^{+0.6}_{-0.0}$	$^{+4}_{-2}$	$^{+0}_{-12}$	$^{+6}_{-6}$